



ALGERIAN DEMOCRATIC AND POPULAR REPUBLIC
MINISTRY OF HIGH EDUCATION AND SCIENTIFIC RESEARCH

UNIVERSITY OF KASDI-MERBAH OUARGLA

DOMAIN : SCIENCE AND TECHNOLOGIE

FACULTY : APPLIED SCIENCES

FEILD : PROCESS ENGINEERING

SPECIALITY : CHIMICAL ENGINEERING

THEME

**SIMULATION AND OPTIMIZATION OF
SOLAR CELL BASED ON THIN FILM**

PRESENTED BY:

- ✓ ABDERRAZAK BABASIDI
- ✓ ABDELMOUMENE BOUAL

Submitted to the jury composed of :

| | | | |
|---------------|-----|------|------------|
| LATI MOKHTAR | MCB | UKMO | President |
| ATTIA ABBAS | MAA | UKMO | Examiner |
| BACHA OUSSAMA | MCA | UKMO | Supervisor |

UNIVERSITY YEAR : 2021 / 2022

Abstract

Thin film cadmium telluride (CdTe) is the the material for realization of low cost and high efficiency solar cell. The simulation has been performed under the consideration of incident solar radiation of 1kW/m^2 and Air mass of 1.5 and stannic oxide (SnO_2) and silver (Ag) has been considered as the anode and cathode of the CdTe/CDS solar cell respectively. Here, the voltage, current circuit, Fill Factor (FF) and Quantum Efficiency (QE) of the solar cell has been determined and analyzed, we find layer thickness of $4\mu\text{m}$ CdTe, $0.005\ \mu\text{m}$ CDS, electron affinity of 3.5 eV, acceptor concentration of $3 \times 10^{14}\text{cm}^{-3}$. In this work, a conventional structure of CdTe thin film solar cells was investigated and conversion efficiency as high as 16.53% was achieved when thickness of CdS layer is $0.005\ \mu\text{m}$ with the CdTe baseline structure of $\text{SnO}_2/\text{CdS}/\text{CdTe}$. To explore the possibility of thin film and high efficiency CdTe/CDS solar cells. Moreover, it was found that there were scopes to increase cell efficiency by reducing the cadmium sulfide (CdS) window layer thickness. All the simulations have been done under SCAPS simulator.

Keywords: Solar cell, thin film, simulation, CdTe, CDS, SCAPS.

تيلورايد الكاديوم ذو الأغشية الرقيقة (CdTe) هو المادة الرائدة لتحقيق خلية شمسية منخفضة التكلفة وعالية الكفاءة. تم إجراء المحاكاة في ظل مراعاة الإشعاع الشمسي الساقط بمقدار 1 كيلو وات / م² واعتبرت الكتلة الهوائية 1.5 وأكسيد الستانيك (SnO₂) والفضة (Ag) بمثابة الأنود والكاثود للخلية الشمسية CdTe / CDS على التوالي. هنا ، تم تحديد وتحليل الجهد والدائرة الحالية وعامل التعبئة (FF) والكفاءة الكمية (QE) للخلية الشمسية ، ونجد سماكة الطبقة 4 μm CdTe ، 0.005 ميكرومتر CDS ، تقارب الإلكترون 3.5 eV ، في هذا العمل تم فحص البنية التقليدية للخلايا الشمسية ذات الأغشية الرقيقة CdTe وتم تحقيق كفاءة تحويل تصل إلى 16.53٪ عندما يكون سمك طبقة CdS 0.005 ميكرومتر مع بنية CdTe الأساسية لـ SnO₂ / CdS / CdTe. لاستكشاف إمكانية وجود غشاء رقيق وخلايا شمسية CdTe / CDS عالية الكفاءة. علاوة على ذلك ، وجد أن هناك نطاقات لزيادة كفاءة الخلية عن طريق تقليل سماكة طبقة نافذة كبريتيد الكاديوم (CdS). تم إجراء جميع عمليات المحاكاة باستخدام جهاز محاكاة SCAPS.

الكلمات المفتاحية: الخلايا الشمسية ، الأغشية الرقيقة ، المحاكاة ، CdTe ، SCAPS ، CDS

Résumé

Le tellurure de cadmium à couches minces (CdTe) est le principal matériau pour la réalisation de cellules solaires à faible coût et à haut rendement. La simulation a été réalisée avec un rayonnement solaire incident de 1kW/m^2 et d'une masse d'air de 1,5 et l'oxyde stannique (SnO_2) et l'argent (Ag) ont été considérés comme l'anode et la cathode de la cellule solaire CdTe/CDS respectivement. Ici, la tension, le courant de court-circuit, le facteur de remplissage (FF) et l'efficacité quantique (QE) de la cellule solaire ont été déterminés et analysés, nous avons trouvé ces valeurs épaisseur de couche de $4\mu\text{m}$ CdTe, $0,005\mu\text{m}$ CDS, une affinité électronique de 3,5 eV, une concentration d'accepteur de $3 \times 10^{14}\text{ cm}^{-3}$. Dans ce travail, une structure conventionnelle de cellules solaires à couches minces CdTe a été étudiée et une efficacité de conversion aussi élevée que 16,53 % a été obtenue lorsque l'épaisseur de la couche CDS est de $0,005\mu\text{m}$ avec la structure de base CdTe de $\text{SnO}_2/\text{CdS}/\text{CdTe}$. Pour explorer la possibilité de couches minces et de cellules solaires CdTe / CDS à haut rendement, il a également été constaté qu'il était possible d'augmenter l'efficacité des cellules en réduisant l'épaisseur de la couche de fenêtre en sulfure de cadmium (CdS). Toutes les simulations ont été réalisées sous simulateur SCAPS. En outre, il a été constaté que l'efficacité normalisée de la cellule augmentait de manière linéaire avec la diminution de la température de fonctionnement au gradient de 200 K, ce qui indiquait une meilleure stabilité des cellules solaires CdS/CdTe.

Mots clé: cellule solaire, couche mince, simulation, CdTe, CDS, SCAPS.

acknowledgement

First of all, we are thankful and expressing our gratefulness to who offers us His divine blessings, patience, mental and physical strength to complete this work successfully.

Then we want to express my heartfelt gratitude toward my supervisor Dr. oussama bacha for providing us valuable guidance during our work in the Department applied sciences and process Engineering at University of kasdi merbah ouargla. He provided us tremendous freedom to pursue various ideas of our interest as well as nudged we in the right direction with his vision.

His scholarly guidance, important suggestions, endless patience, constant supervision, valuable criticism and enormous amount of work for going through our drafts and correcting them and generating courage from the beginning to the end of the research work has made the completion of the thesis possible. And we would like to thank all members of the examining committee of this work.

We would also thank association sonatrach partamina talisman, for the golden advices about the research fields of the our project topic and for suggesting we corrections at some important points in the drafts of the work.

Last but not the least ; we are highly grateful to our parents and family members for their support, innumerable sacrifice, unconditional love, unwavering faith and constant encouragement, which have always been a source of great inspiration for us.

List of tables

| | |
|--|----|
| Table I. 1: Solar cell efficiencies achieved by the principal semiconductor technologies. | 10 |
| Table III.1: Some of the properties of CdTe/CdS thin films solar cells | 35 |
| Table III. 1: Original case Performance of CdTe/CDS thin film Solar Cell | 45 |
| Table III. 2: Performance of CdTe /CDS thin film Solar Cell for varying CdTe layer thickness | 46 |
| Table III. 3: Performance of CdTe/CDS thin film Solar Cell for varying CDS layer thickness | 46 |
| Table III. 4: Performance of CdTe/CDS thin film Solar Cell for varying CDS layer electron affinity | 46 |
| Table III. 5: Performance of CdTe/CDS thin film Solar Cell for varying CdTe layer acceptor concentration | 46 |

List of figures

| | |
|--|----|
| Figure I. 1: thin film | 3 |
| Figure I. 2: Application of thin film for solar cell | 6 |
| Figure I. 3: Single Crystal solar cells in panel | 7 |
| Figure I. 4: Amorphous-Si solar panel | 8 |
| Figure I. 5: The structure of a typical crystalline silicon solar cell | 9 |
| Figure I. 6: Best research cell efficiency up to 2020 | 12 |
| Figure I. 7: Structure of a thin-film solar cell | 13 |
| Figure I. 8: characteristics of a solar cell | 15 |
| Figure I. 9: Photovoltaic materials | 17 |
| Figure II. 1: Picture of AMPS Program | 22 |
| Figure II. 2: Picture of wxAMPS program | 23 |
| Figure II. 3: Main window of PC1D | 24 |
| Figure II. 4 :graphical interface of AFORS-HET | 25 |
| Figure II. 5: The SCAPS start-up panel(the Action panel or main panel | 26 |
| Figure II. 6: Define the working point | 27 |
| Figure II. 7: SCAPS panels | 28 |
| Figure II. 8: Batch calculation | 29 |
| Figure II. 9: Defining a solar cell structure | 30 |
| Figure II. 10: Examples of visualization of the solar cell parameters | 31 |
| Figure II. 11: Ordinate choices on the QE-panel | 31 |
| Figure III. 1: Structure of the CdS/CdTe,As solar cells studied | 33 |

| | |
|---|----|
| Figure III. 2: Effect of CdTe thickness on the quantum efficiency | 34 |
| Figure III. 3: Effect of the CdTe film thicknesses on cell performance | 37 |
| Figure III. 4: Effect of CdTe thickness on the quantum efficiency | 38 |
| Figure III. 5: Effect of the CDS film thicknesses on cell performance | 39 |
| Figure III. 6: Effect of CdS thicknesses on the cell QE | 40 |
| Figure III. 7: Effect of the CDS electron affinity on cell performance | 41 |
| Figure III. 8: Acceptor concentration (NA) profile for px CdTe | 42 |
| Figure III. 9: Effect of the CdTe film acceptor concentration on cell performance | 44 |
| Figure III. 10: Effect of CdTe acceptor concentration on the cell QE | 45 |
| Figure III. 11: Effect of operating temperature on the normalized cell efficiency | 45 |

LIST OF ABBREVIATIONS

| | |
|-----------|--|
| AFORS-HET | AUTOMAT FOR SIMULATION OF HETERO STRUCTURES |
| AMPS | ANALYSIS OF MICROELECTRONIC AND PHOTONIC STRUCTURES |
| AM | AIR MASS |
| ASA | ADVANCED SEMICONDUCTOR ANALYSIS |
| CV PANEL | CAPACITANCE AND CONDUCTANCE AS A FUNCTION OF APPLIED VOLTAGE |
| CDTE | CADMIUM TELLURIDE |
| CDS | CADMIUM SULFIDE |
| FF | FILL FACTOR |
| JSC | SHORT CIRCUIT CURRENT DENSITY |
| IV PANEL | INDICATOR CURRENT-VOLTAGE SIMULATIONS PANEL |
| PCID | PROGRAM FOR IBM-COMPATIBLE PERSONAL COMPUTERS |
| PSCs | PERFORMANCE SOLAR CELLS |
| PV | PHOTOVOLTAIC |
| QE | QUANTUM EFFICIENCY |
| SCAPS | ONE DIMENSIONAL SOLAR CELL SIMULATION PROGRAM DEVELOPED |
| SNO2 | SANNTIC OXIDE |
| TCO | TRANSPORT CONDUCTING FILMS |
| VOC | CIRCUIT VOLTAGE |

Table of contents

| | |
|---|-----------|
| Abstract | I |
| Acknowledgement | IV |
| List of tables | V |
| List of tables | VI |
| List of figures | VII |
| List of abbreviations | IX |
| Introduction | 1 |
| I .1 Thin film | 3 |
| I.1.1 Definition | 3 |
| I.1.2 Properties..... | 4 |
| I.1.2.1 Reflectivity and Transmission..... | 4 |
| I.1.2.2 Ellipsometry | 4 |
| I.1.2.3 Scattering..... | 4 |
| I.1.2.4 Color..... | 4 |
| I.1.3 Application | 5 |
| I.1.3.1 . Medical applications | 5 |
| I.1.3.2 . Environmental applications..... | 5 |
| I.1.3.3 . Photovoltaic | 6 |
| I.1.3.4 . Flat panel displays | 7 |
| I .2 Solar cells | 7 |
| I.2.1 Different characteristics of solar cells | 7 |
| I.2.2 photovoltaics cells technologies..... | 11 |
| I.2.2.1 Crystalline silicon solar cells | 12 |
| I.2.2.2 Thin-film solar cells..... | 12 |
| I.2.2.3 Recent advances in solar cells | 13 |
| I .3 Photovoltaics cells based on thin films | 13 |

| | |
|---|-----------|
| I.3.1 Historical | 13 |
| I.3.2 Principle of operation..... | 14 |
| I.3.3 Photovoltaic cell materials | 16 |
| I.3.4 Performance and efficiency..... | 17 |
| II .1 Basic Parameters of Solar Cell | 19 |
| II.1.1 Open-circuit voltage (VOC) | 19 |
| II.1.2 Short-circuit current (JSC)..... | 19 |
| II.1.3 Fill Factor | 19 |
| II.1.4 Quantum Efficiency..... | 20 |
| II .2 Simulation and optimization of solar cell..... | 20 |
| II.2.1 Definitions..... | 21 |
| II.2.1.1 Simulation | 21 |
| II.2.1.2 Optimization..... | 21 |
| II.2.2 Simulation and optimization of softwares | 21 |
| II.2.2.1 AMPS | 21 |
| II.2.2.2 wxAMPS | 22 |
| II.2.2.3 PC1D..... | 23 |
| II.2.2.4 AFORS-HET | 24 |
| II.2.2.5 ASA | 25 |
| II.2.2.6 SCAPS 1D | 25 |
| II .3 Simulation and Optimization by SCAPS | 26 |
| II.3.1 Basics | 26 |
| II.3.2 Conditions of scaps | 27 |
| II.3.2.1 the temperature..... | 27 |
| II.3.2.2 the illumination | 27 |
| II.3.3 Define the problem | 27 |
| II.3.4 Select the measurement(s) to simulate | 27 |
| II.3.5 Start the calculation(s) | 28 |
| II.3.6 Display the simulated curves | 28 |
| II.3.7 Editing the problem..... | 29 |
| II.3.8 Speeding up: Batch calculation | 29 |

| | |
|--|-----------|
| II.3.8.1 Speeding up: Recorder | 29 |
| II.3.9 Editing a solar cell structure | 29 |
| II .4 Measurement specific options | 30 |
| II.4.1 The IV-panel | 30 |
| II.4.2 The CV-panel..... | 31 |
| II.4.3 The QE-panel | 31 |
| III .1 CdTe over time | 32 |
| III .2 Device Modeling and Simulation..... | 33 |
| III .3 Results and discussion..... | 36 |
| III .3.1 Influences of thiknees of CdTe | 36 |
| III .3.2 Influences of thiknees of CDS | 38 |
| III .3.3 Influences of electron affinityof CDS | 40 |
| III .3.4 The Influences of acceptor concentration of CdTe layer..... | 42 |
| Conclusion..... | 48 |
| Bibliography..... | 49 |

Introduction

The sharp rise in energy prices has heightened interest in renewable energy sources, particularly solar cells. This can be seen in the significant expansion of research in this field. Thin-film solar cells still have the potential to lower production costs. Several optimization strategies have been presented to boost the conversion efficiency of thin film solar cell. The employment of compositionally graded profiles in the structure of solar cell is one of the promising ways for improving the performance of third generation solar cells. The grading of bandgaps and other semiconductor characteristics, in particular Doping concentration was proposed a long time ago to boost solar efficiency. both experimentally and by computer simulation. appropriate substances to implement band-gap engineering in graded solar cells.

In this work, we tested the performance parameters of the CdTe/CDS thin film Solar cell which has been analyzed by studying the characteristics of the layers using numerical simulation.

Variations in layer thickness, electron affinity, and acceptor concentration were used to investigate the properties of the CdTe/CDS cell. The form factor (FF) and external quantum efficiency (EQE) of the layers have been determined and examined in each of these examples. The simulation was carried out with incident solar radiation of 1kW/m^2 irradiance and an air mass of 1.5, with stannic oxide (SnO_2) and silver (Ag) serving as the anode and cathode of the CdTe/CDS solar cell respectively, from the simulation and optimization what is the highest efficiency of CdTe/CDS thin film solar cell which can be produced And what is the relation between the performance parameters and efficiency.

This thesis is divided into tree chapters:

- I. The chapter 1 presents an overview on thin films especially in properties and applications and a preface in different characteristics of solar cells .Secondly, supplys an overview on historical photovoltaics based on thin films and there the prinsipal of operation materials,performances and efficiency.
- II. The chapter 2 presents a basic parameters of solar cells, and supplys a different simulation softwares for thin films solar cells, in our work we used the **scaps** which has been measure the performance of solar cell (QE, FF, Voc, Jsc).

III. The chapter 3 talk about structure of the studied cell (CdTe/CDS) especially , the influences: thickness CdTe, thickness CDS, electron affinity of CDS and acceptor concentration.

I .1 Thin film

1.1.1 Definition

A thin film, according to them, is a material that is produced by the random nucleation and growth processes of individually condensing/reacting atomic/ionic/molecular species on a substrate. The structural, chemical, metallurgical, and physical properties of such a material are highly influenced by a variety of deposition parameters, and thickness may also be a factor[1]. Thin films can range in thickness from tens to thousands of nanometers. One may obtain a thin material (not a thin film) by a number of other methods (normally called thick-film techniques) such as by thinning bulk material, or by depositing clusters of microscopic species in such processes as screen-printing, electrophoresis, slurry spray, plasma gun, ablation, etc. The given definition still leaves room for a broad field of technologies to deposit the thin film (plasma, sputtering, evaporation, deposition from the liquid phase, etc.) and to tailor its electrical and morphological properties (crystalline, amorphous and intermediary forms). These techniques and their relation with the final morphology and the photovoltaic performance will be discussed in the separate chapters dealing with the different thin film solar cell technologies[2].

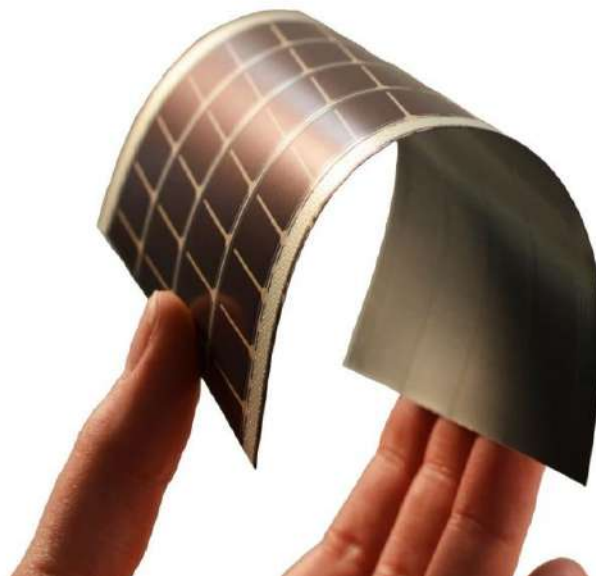


Figure I. 1: thin film[3].

1.1.2 Properties

1.1.2.1 Reflectivity and Transmission

The reflectivity of a substrate covered with a thin film depends on the wavelength according to Fresnel's laws. As a consequence, also the transmission is wavelength dependent. The thin film parameters determining the reflectivity are the film thickness and the complex index of refraction nQ , which is determined by the index of refraction n and by the absorption coefficient B according to Beer's absorption law[4].

1.1.2.2 Ellipsometry

When polarized light is reflected at a surface, the polarization state changes depending on the thickness, the index of refraction and the absorption coefficient of the thin film and the substrate. Ellipsometry is a technique that can measure these parameters with high accuracy. The optical Properties of Thin Films principle is rather simple. The change of the polarization state of a light beam incident onto the sample is measured after the reflection. The adequate formalism to describe the phenomena associated with ellipsometry is the Jones and Stokes formalism of polarization[5].

1.1.2.3 Scattering

Besides reflectivity, absorption and transmission thin films can also be characterized by their scattering properties. In terms of ray optics scattering can be described as the stochastic change of the propagation direction of a light ray at the surface interface. Even if the surface is not actually reflective there is always the specular ray, which changes its direction according to the reflection law. Scatter Models. Scatter models are defined in terms of an intensity probability distribution function. When a ray is scattered, a new direction of propagation is chosen. When a beam scatters, a new propagation direction is determined[6].

1.1.2.4 Color

The color of thin films is determined by the spectrum of the reflected or transmitted light. Color is strictly speaking not a pure physical quantity but related both to physics and subjective perception. However, it is possible to attribute to each color a set of values which can be related to the measurable light spectrum. The procedure how to calculate these color coordinates from a given light spectrum is regulated in various international standards. The CIE (1932) standard is the most widely used[7].

1.1.3 Application

1.1.3.1 Medical applications

The use of thin films for medical applications arises from the fact that most bulk biomaterials that are currently used as invasive devices were not developed for this specific purpose. In fact, most bulk materials used as biomaterials can be found in our garages because they were developed for different purposes. Examples are light titanium alloys used in cars parts or carbon reinforced composites in bicycles. The utilization of thin films in medical applications stems from the fact that most bulk biomaterials utilized as invasive devices today were not designed for this purpose. In reality, because they were designed for various reasons, most bulk materials utilized as biomaterials may be found in our garages. Light titanium alloys are employed in vehicle parts, and carbon reinforced composites are used in bicycles. The experience has proven that the body more or less tolerates these materials and their overall set of properties/characteristics (mechanical, electrical, etc.) is appropriated for a specific use inside the body[8].

1.1.3.2 Environmental applications

The use of thin films in the design of biotools for environmental application is here illustrated by two case studies. The first describes the development of an arsenic biofilter. The environmental contamination with arsenic is a worldwide problem, and the development of new strategies for arsenic removal is an ever ongoing research. In this study, genetically modified bacteria able to accumulate arsenic were generated by modification of the arsenic resistant strain *Ochrobactrum tritici* SCII24T. The *O. tritici* As5 mutant cells, exhibiting a high percentage of arsenite accumulation, were immobilized on a commercial polyethylene (PE) net after sputtered modified by the deposition of poly(tetrafluoroethylene) (PTFE) thin films, with approximately 500 nm thick. Different PTFE thin films were tested regarding their ability to immobilize cells in an active form that enabled the microorganisms to form a biofilm and work as a biofilter for arsenic. The surface that exhibited a mild zeta potential value, hydrophobic characteristics, the lowest surface free energy but with a high polar component and the appropriate ratio of chemical reactive groups showed to be the optimal for bacteria development. The immobilized cells maintained their ability to accumulate the surrounding arsenite[9].

I.1.3.3 Photovoltaic

Adam and Day were the first to investigate the photovoltaic effect in solids in 1876, when they created a solar cell out of selenium with a 1–2% efficiency. Albert Einstein's photon theory described the photovoltaic effect in 1904. The development of a technology to generate pure crystalline silicon by Polish scientist Jan Czochralski in 1916 was a crucial milestone in contemporary electronics[10]. Due to high device prices, early attempts to make photovoltaic cells a viable form of power generation for terrestrial applications failed. In many countries, the "energy crisis" of the 1970s sparked a fresh wave of projects to make solar systems more cheap, particularly for off-grid applications[11]. The dramatic decreases in solar cell pricing in recent years have reignited interest in the technology for example, since 2000, yearly growth in PV system manufacturing has topped 40%, and total installed capacity globally has reached roughly 22 GW[12].



Figure I. 2: . Application of thin film for solar cell[13].

I.1.3.4 Flat panel displays

The production of Flat Panel Displays (FPDs) is one of the most competitive and technologically sophisticated industries in the world. Device designers and engineers are always working to meet the global customer demand for larger displays, higher pixel

resolution, and feature-rich performance at a cheaper cost than earlier generations of technology. Contamination management in air, gas, and liquid process streams is increasingly a top priority for process engineers and designers[14].

I .2 Solar cells

1.2.1 Different characteristics of solar cells

Single crystal wafers, polycrystalline wafers, and thinfilms are used in the fabrication of silicon solar cells. Shredding single crystal wafers (approximately 1/3 to 1/2 millimeter thick) from a big single crystal bullion stretched out at roughly 1400 °C is an extremely costly procedure. To absorb sunlight, silicon must be of extremely high purity and have a nearly flawless crystal structure[15].

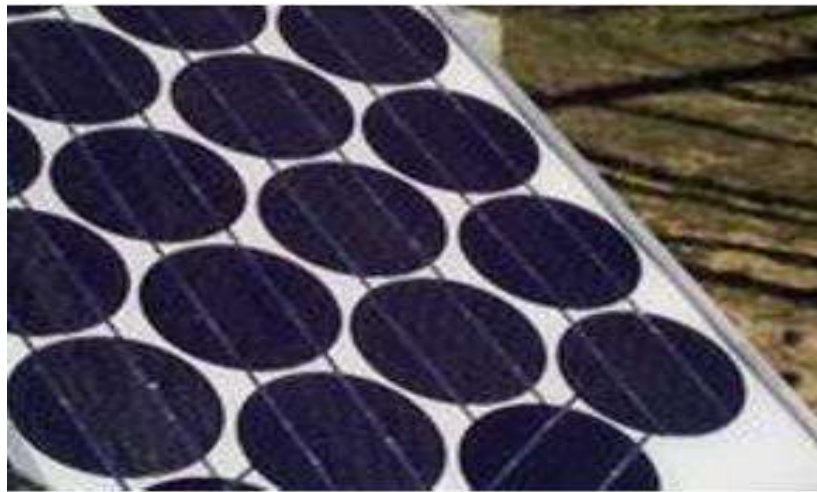


Figure I. 3: Single Crystal solar cells in panel[16].



Figure I. 4: Amorphous-Si solar panel[16].

Because the efficiency of crystalline silicon cells is closely tied to the efficiency of solar systems, it dominates the photovoltaic industry. However, though single crystals are more efficient, cells are now frequently constructed using multicrystalline material rather than single crystals to save money. It may be argued that crystalline silicon cell technology is well established because the modules have a long lifetime (20 years or more) and their greatest manufacturing efficiency is nearing 18 percent. Furthermore, amorphous silicon solar cells are less expensive but less efficient than other types of silicon cells. Amorphous thin films are used to make silicon solar cells, which are used to power a range of consumer items. With the advancement of the solar industry, larger amorphous silicon solar modules are becoming accessible. A novel form of thin film module is shown in Figure 1-4. High-efficiency solar cells design from gallium arsenide, indium phosphide or their derivatives are used in specialized applications such as to power satellites or in systems which operate under high-intensity concentrated sunlight.

In Figure I-5 shows below the structure of a typical silicon solar cell. The electrical current generated in the semiconductor is extracted by contacts to the front and back of the cell. As can be seen at the top, the finger contact arrangement should enable light to travel through while supplying current to a bigger bus bar. A variety of thin film devices employ transparent conducting oxide[17]. When solar cell absorbing the sunlight meantime it should be minimize the reflection of light in order to increase the efficiency. This is called the antireflection coating (ARC) which is covered with a thin layer of dielectric material[16].

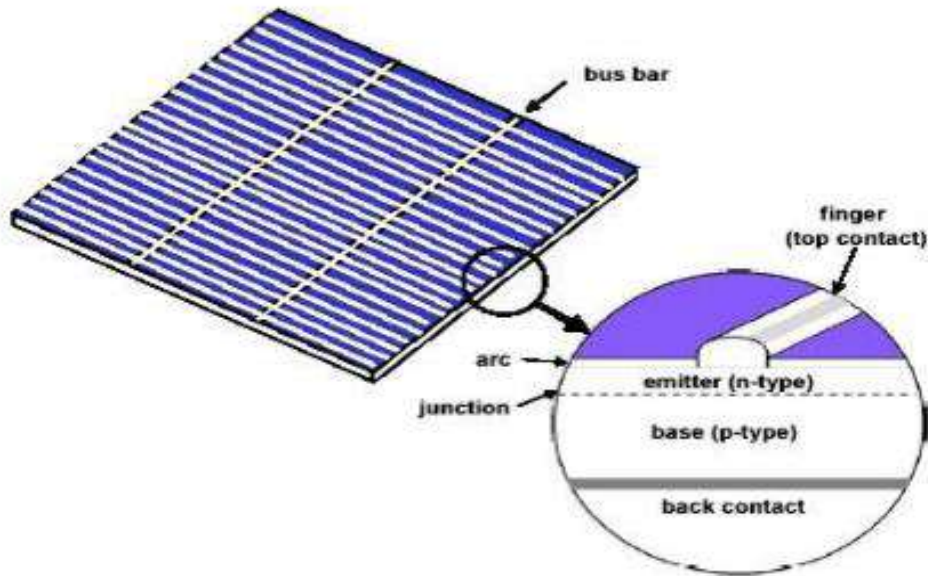


Figure I. 5: The structure of a typical crystalline silicon solar cell[16].

The energy transformation in solar cells is different from the classical heat engine process, so the limitations and losses that occur in more detail. The fundamental mechanisms responsible for losses in solar cells are explicit from the discussion of solar cell operation. A considerable part of the solar spectrum is not utilized because of the inability of a semiconductor to absorb the below-band gap light which causes from the heat is produced on carrier generation in the semiconductor by photons with energy in excess of the band gap. Losses can be decreased by using a device known as a tandem cell, which is made up of multiple semiconductors with varying band gaps[15].

The top cell of a tandem is comprised of a semiconductor with a large band gap, which transforms short wavelength light. The bottom cell converts the light that has been transferred. This change reduces the system's efficiency by a significant amount[15].

Other losses reduce the efficiency of devices, 50% is the achievable at maximum, some thin film devices it is less. Non-radiative recombination of the photo generated electron hole pairs is the common loss mechanisms which is present in all practical devices. Pollution or impurities, flaws in the crystal structure, or at the surface of the semiconductor, where energy levels may be injected inside the energy gap, are the most typical causes of recombination.

These levels act as stepping stones for the electrons to fall back into the valence band and recombine with holes. Measures taken to minimize the recombination losses include careful processing to maintain long minority carrier lifetime, and protecting the external surfaces of the semiconductor by a layer of passivating oxide to reduce surface recombination[15].

Measures take in to minimize the recombination losses include careful processing to maintain long minority carrier lifetime, and protecting the external surfaces of the semiconductor by a layer of passivating oxide to reduce surface recombination[15].

The contacts can be surrounded by strongly doped areas that operate as "minority carrier reflectors," preventing minority carriers from reaching and recombining with the contacts. The losses to current at the interface are sometimes bundled under the phrase "collection efficiency," which is defined as the ratio of the number of carriers created by light to the number that reaches the junction. Considerations of the collection efficiency affect the design of the solar cell. In crystalline materials, the transport properties are usually good, and carrier transport by simple diffusion is sufficiently effective. Electric fields, on the other hand, are required to draw the carriers in amorphous and polycrystalline thin films. After that, the junction region is widened to absorb the majority of the photon flow.

Light reflection from the top surface, shadowing of the cell by the top contacts, and partial absorption of light are all sources of current losses in the cell. Because silicon is an indirect-gap semiconductor, it has poor light absorption characteristics. This last attribute can be especially important for crystalline silicon cells. The use of multi-layer antireflection coatings, surface texturing to generate tiny pyramids, and making the back contact optically reflective are all options for reducing these losses. When combined with a textured top surface, this geometry results in effective light trapping which provides a good counter measure for the low absorptivity of silicon. Top-contact shading is reduced in some cells by forming these contacts in narrow laser grooves, or all the contacts can be moved to the back of the cell. Another loss in commercial cells is ohmic losses in the transmission of the current produced by the solar cell, usually grouped together as a series resistance, which reduce the fill factor of the cell. The principal characteristics of different types of cell in or near commercial production are summarized in table I-1 below[15].

Tableau I. 1: Solar cell efficiencies achieved by the principal semiconductor technologies.

| Material | Area(cm) | Best efficiency (%) | Technology |
|------------------------------|----------|----------------------|-------------|
| Mono or multi cryst. Silicon | 10 | 25 | Plate/wafer |
| Amorphous silicon | 5 | 13 | Thin film |
| Copper indium dieseline | 8 | 16 | Thin film |
| Cadmium telluride | 7 | 16 | Thin film |

In addition, to crystalline silicon, much effort is focused on the manufacture of thin film devices which have lower material requirements. Furthermore, there is considerable research activity in purely molecular materials and photovoltaic materials are no longer dependent onto semiconductors. A number of research groups have showed solar cells based on conducting polymers, often in combination with fullerene derivatives as electron acceptors to create the p-n junction. There is much to look forward to if their success matches the achievements of the LED technology. Amorphous silicon is one of a number of thin film technologies. This form of solar cell may be put on low-cost substrates like glass or plastic as a film. Thin multicrystalline silicon, copper indium dieseline/cadmium sulphide cells, cadmium telluride/cadmium sulphide cells, and gallium arsenide cells are some of the other thin film technologies. Thin film cells provide a number of advantages, including simplicity of deposition and assembly, the ability to be placed on low-cost substrates or construction materials, mass manufacturing ease, and high adaptability for big applications[18].

1.2.2 photovoltaics cells technologies

PV technology benefits from the microelectronics and display industries extensive expertise bases: For CIS and CdTe, however, there is no such synergy. These technologies production hazards and ecological balance sheet should also be considered. The argument for silicon is well-established and well-documented, but the PV community lacks access to independent and in-depth investigations on CIS and CdTe conducted by professional ecotoxicological organizations. Finally, due to the advent of effective low-cost light trapping methods, it is no longer required to utilize a direct-bandgap semiconductor in a thin-film PV solar cell to achieve sufficient optical absorption[12].

1.2.2.1 Crystalline silicon solar cells

Single junction solar cells based on silicon wafers along with single crystal and multicrystalline silicon oversee recent solar photovoltaic development. This sort of single-junction, silicon wafer system is now frequently referred to as the first generation of solar PV technology, much of which was based on screen-based systems comparable to those shown in fig 1-6[19].

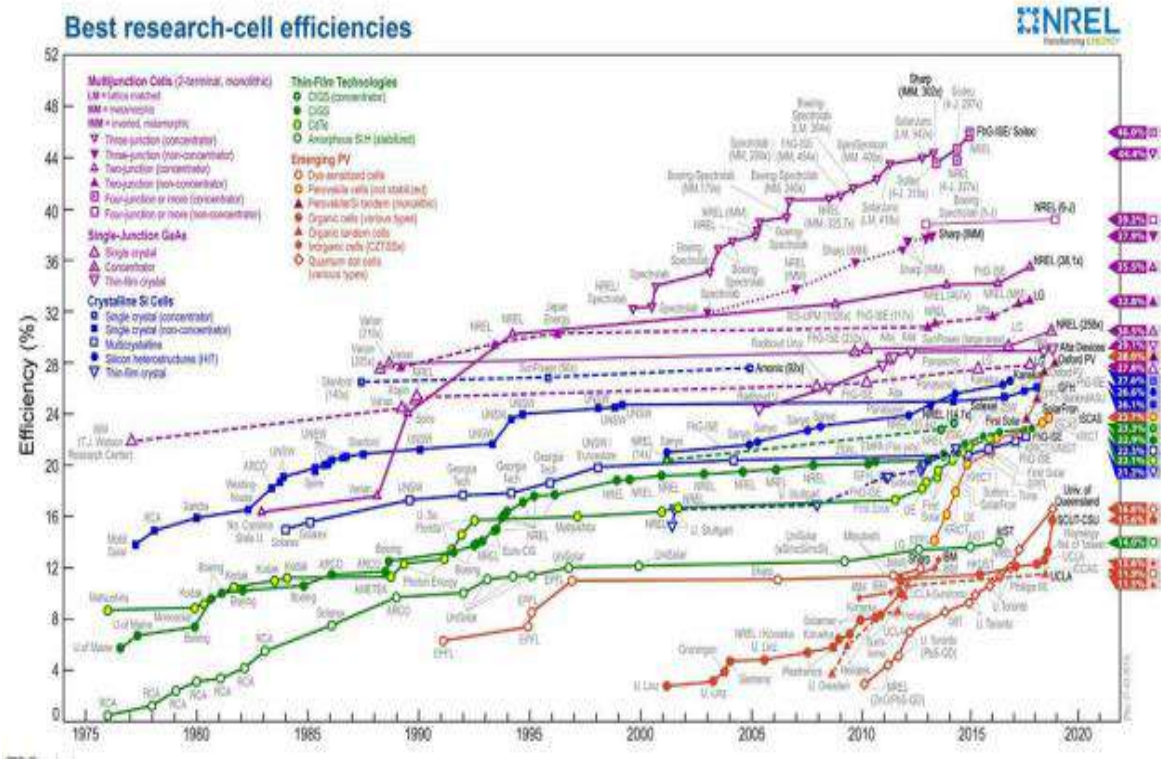


Figure I. 6: Best research cell efficiency up to 2020[20].

1.2.2.2 Thin-film solar cells

The second generation of solar cells is known as thin-film solar cells. A structural view of a thin-film solar cell is shown in Figure 1-8. These solar cells are less expensive than silicon crystalline solar cells, yet they have shown to be more effective[19]. A thin layer of semiconductor PV material is put over the metal, glass, or plastic foil in such cells. Due to the

nonsingle-crystal structure, thin films have a low efficiency and require a larger range of fields, which increases associated expenditures such as mounting[19].

Amorphous silicon (a-Si), cadmium telluride (CdTe), copper indium gallium selenide (CIGS), polymer, and organic solar cells are examples of thin-film solar cells for outdoor application[11].

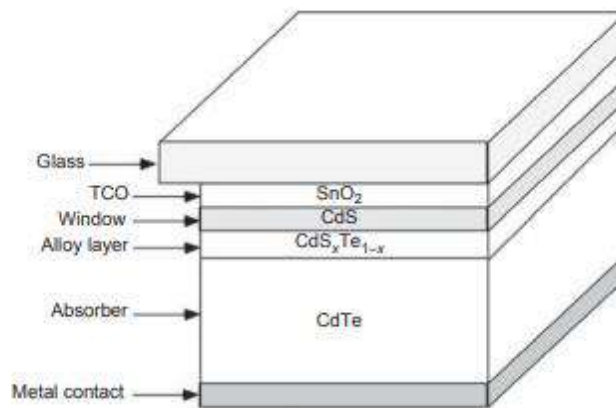


Figure I. 7: Structure of a thin-film solar cell[21].

1.2.2.3 Recent advances in solar cells

There has been continuous progress in the use of renewable energy in a wide spectrum and solar energy in a diligent manner for useful applications. Various innovative solar cells, such as gallium arsenide, perovskite, and dye-sensitized solar cells, have recently been developed[19].

I .3 Photovoltaics cells based on thin films

1.3.1 Historical

Edmond Becquerel discovered the photovoltaic (PV) phenomenon in 1839. It remained a scientific phenomenon with limited device applications for a long period. Silicon PV diodes became available after silicon was introduced as the primary semiconductor material in the late 1950s. They quickly became indispensable for supplying electrical power to satellites and telecommunications equipment in remote regions[11].

Then, in the 1970s, a fundamental shift in public understanding of the energy supply problem occurred: the 1973 oil crisis raised public awareness of fossil fuel limitations, and many governments (including those of the United States, Japan, and numerous European countries) began to take action. Several years later, significant efforts to find alternate energy sources, notably PV solar energy, were launched. This tendency was fueled by public outrage over nuclear fission reactors, as well as a series of nuclear power plant disasters, most notably Three Mile Island in 1979 and Chernobyl in 1986[22]. The current cost of electricity generated by PV systems is around an order of magnitude greater than the current market prices of electricity generated by hydraulic power, nuclear, and fossil fuels (except in remote places). It looks to be extremely difficult to significantly enhance the energy conversion efficiency of low-cost PV modules over 15% at this time due to physical constraints. As a result, huge areas must be set aside for PV electricity generation. The cost of PV solar installations is determined by the size of the installation and the supporting structures. PV installations must be fully integrated into the existing environment and habitat to achieve this. Although solar cells and PV installations do not emit CO₂ during operation, they do consume a lot of energy and produce CO₂ and other pollutants during manufacturing, solar modules and PV installations' energy payback time and ecological balance sheet are thus crucial factors to consider when selecting a future technology[22].

1.3.2 Principle of operation

A semiconductor diode is the foundation of a PV solar cell. Incoming photons are absorbed and converted into electron-hole pairs by the semiconductor material. The semiconductor's bandgap energy E_{gap} is the most important factor in this photo generation stage. No photons with an energy $h\nu$, E_{gap} will contribute to photo generation in an ideal instance, whereas all photons with an energy $h\nu$ will contribute to photo generation. E_{gap} will each contribute E_{gap} of energy to the photo generated electron-hole pair, with the excess energy ($h\nu - E_{gap}$) being dissipated relatively quickly due to the normalization. The flux of photons with an energy of $h\nu$. E_{gap} determines the maximum limit for photo generated electric current density J_{ph} . As the bandgap E_{gap} grows larger, J_{ph} drops. The net energy delivered to each electron-hole pair grows at the same time, There is a "optimum" for E_{gap} (≈ 1.1 eV) at which the highest amount of energy from incident sunlight can be transmitted to the totality of photo generated electron-hole pairs. Approximately half of the incident solar energy is transferred at this bandgap. Only if optical losses due to reflections, shading by grid

patterns, and other factors are minimized, as well as if the semiconductor is thick enough to absorb all usable incident photons, can this limit be approached. Because of the low levels of absorption coefficients in semiconductors with an indirect bandgap (such as crystalline silicon), the latter criterion is more difficult to meet, but it is more advantageous in amorphous semiconductors or semiconductors with a direct bandgap. As a result, crystalline silicon can only be used for solar cells if it is either relatively thick (100 μm) or if sophisticated light-scattering (light trapping) schemes are used; this is one of the reasons why thin-film crystalline silicon solar cells have only recently begun to be researched on a large scale separation of charges. Because of the internal electric field formed by the solar cells diode structure, the photo generated electron-hole pairs are split in the second step of the energy conversion process, with electrons floating to one electrode and holes drifting to the other electrode. In principle, the diode's dark (non illuminated) properties and the photo generated current can be linearly stacked (1, 2), yielding the solar cell equivalent circuit shown in Fig. and the current-voltage (I-V) curve at the output of a solar cell, shown in Fig. Maximum power can be retrieved from the solar cell at the maximum power point MPP, which is equivalent to the product of the open-circuit voltage V_{oc} times the short-circuit current density J_{sc} times the fill factor FF (FF expresses the form of the I-V curve). J_{sc} , V_{oc} , and FF are the three key parameters characterizing solar cell performance. The maximum limit for J_{sc} is given by the photo generated current density J_{ph} [22].

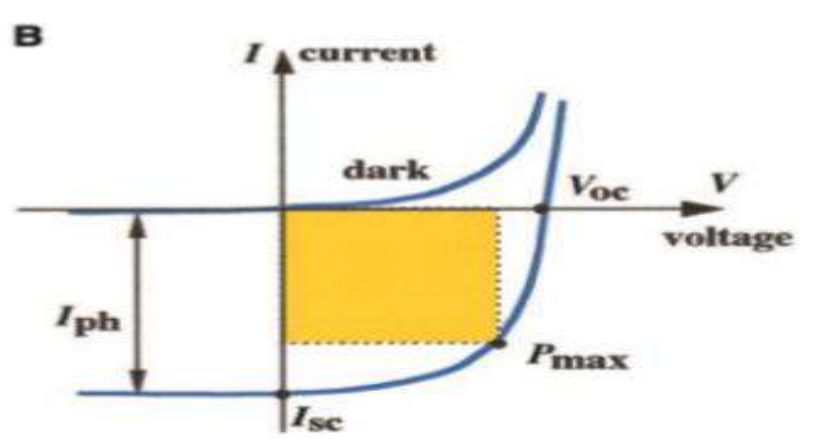


Figure I. 8: characteristics of a solar cell[22].

1.3.3 Photovoltaic cell materials

The materials that have played a major role in photovoltaic solar energy conversion Single crystal materials may be useful in high technology, relatively expensive cells to be used with concentration of sunlight In single crystal form only Si, GaAs, InP, CdTe and CuInSe_2 can be used in photovoltaic devices to produce efficiencies greater than 10 %, and of these only Si and GaAs, and solid solutions based on them, are considered seriously for terrestrial applications. This situation calls attention to the importance of thin - film technology in producing thin film photovoltaic cells for terrestrial applications .In thin film form, CdTe and CuInSe_2 are the leading candidates for solar cell applications. The thin film technology used must pay particular attention to the processing costs associated with large area production. Not only are thin films. needed for the active solar cell layers themselves, they are also needed for win dow materials, anti reflection coatings, passivating coatings, and transparent conducting contacts (CdS, ZnCdS , ZnO, SnO, SnO_2 , In_2O_3 , and indium tin oxide (ITO)).

Decisions have been needed on whether to produce these films by one of the standard methods such as vacuum evaporation , non - reactive or reactive sputtering , electron - beam evaporation , molecular beam epitaxy , and chemical vapor deposition , or by one of a set of developing techniques , such as close - spaced vapor transport (Nicoll, 1963 Saraie et al 1972 Yoshikawa and Sakai, 1974Buch et al, 1977), spray pyrolysis (Chamberlin and Skarman, 1066 Ma et al 1077. Ma and Ruhe 1077) and electrochemical donosition or plating (Panicker et al, 1978).

The references cited here indicate some of the earlier investigative work more recent work is described in the following chapters. An assessment of polycrystalline thin films for solar cell applications : as of 1982 is summarized by Rothwarf (1982) Because of the limited number of different materials, research has attemp ted to broaden the range of possible materials by focusing on solid solutions between these and related materials : Si, C, H, Si, Ge, H, Cu, Agi, InSe_2 , CuGa Ini Sez, GalnP_2 , Zn, CdTe, and Mn, Although in prin ciple it is possible to design " ideal " photovoltaic systems with ideal band gap and no lattice mismatch at heterojunction interfaces, by resorting to more complicated ternary, quaternary, pentenary, and even more complex systems, the materials problems entering in these more complex systems appear to be a serious limitation. A major attempt at increasing efficiency with the limited number of mate- rials available has led to the development of multijunction cells, in

which two (or more) different cells are used together in series to more efficiently absorb the light. Although the measured efficiency for such a multijunction cell can be expected to exceed that of either cell used separately, it is clear that efficiencies do not simply add in such a multijunction cell, since only a fraction of the incident light reaches the lower cell. The ideal situation would be to use a large number of such cells in a multijunction such that each cell could effectively absorb light only within a narrow range of its band gap. Examples of early multijunction cells with two components, and the efficiencies achieved are: GaAs/Si (31%) (Gee and Virshup, 1988), GaAs/CuInSe₂ (21.3%) (Stanbery et al, 1977 Kim et al, 1988), AlGaAs/GaAs (24-28%) (Lewis et al, 1988 Virshup et al, 1988, MacMillan et al, 1989), a-Si:H/CuInSe₂ (15.6%) (Mitchell et al, 1988), a-Si:H/a-Si:Ge:H (13.6%) (Guha 1989), GaInP₂/GaAs (25%) (Olson et al, 1989). As we shall see in our later discussions, the structural complexity of even these two-component multijunction cells is often not trivial[23].

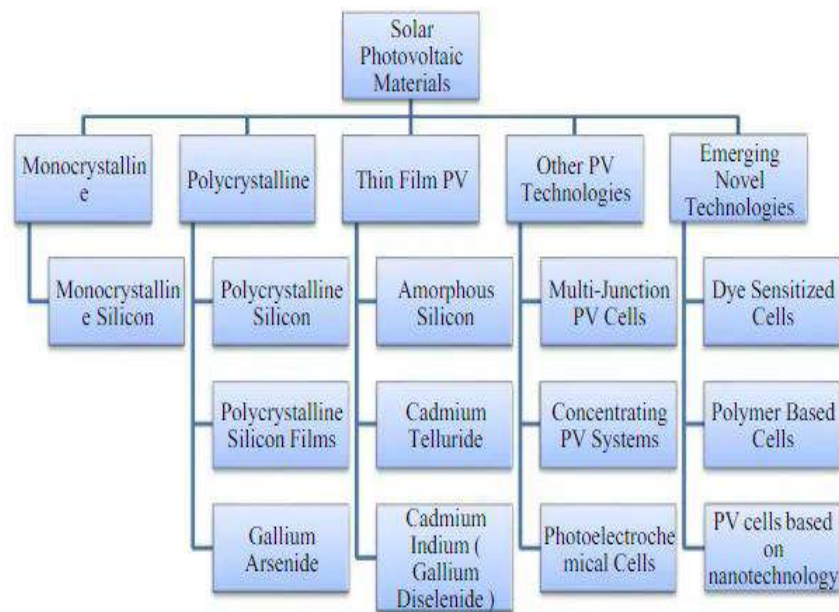


Figure I. 9: Photovoltaic materials[23].

1.3.4 Performance and efficiency

Efficiency must be measured properly since it is critical for characterizing and evaluating the performance of solar devices. Efficiency results have been contentious in the past, and to some extent still are now. The light source used to illuminate the cell is the most critical factor determining the accuracy of the efficiency measurements. A light source with a well regulated spectrum is often used. This so called solar simulator must be accurately

duplicated by each group who hoping to make the measurement, or critical correction factors must be applied that take into account a number of factors characterizing the differences in spectral quality among the various solar simulators. For each photovoltaic material the simulator must duplicate what the cell experiences in the real world under natural sunlight. Control solar cells can be very helpful in correcting for the material differences. Besides, one must accurately know and be able to duplicate from measurement to measurement the density of the light and the junction temperature. Another critical factor in determining the accuracy of an efficiency measurement is that the definition of the area of the cell, as the short circuit current measurement is strongly dependent on the cell area. Much discussion has gone into determining whether the total area.

II .1 Basic Parameters of Solar Cell

II.1.1 Open-circuit voltage (VOC)

The open-circuit voltage VOC is the voltage across the solar cell when $J = 0$, which is the same as the device being open-circuited. Because $J = 0$ and power is the product of current and voltage, no power is actually produced at this voltage. However, the VOC marks the boundary for voltages at which power can be produced. The open-circuit voltage can also be thought of as the point at which the photocurrent generation and dark current processes compensate one another [1].

II.1.2 Short-circuit current (JSC)

Similar to VOC, the short-circuit current density JSC is the current density when $V = 0$, which is the same conditions as the two electrodes of the cell being short-circuited together. Again, there Basics of Photovoltaic Cell is no power produced at this point, but the JSC does mark the onset of power generation. In ideal devices, the JSC will be the same as the photocurrent density J_{ph} . However, it will be seen later that several effects can lower the JSC from this ideal value. Although JSC is technically a negative number with the conventions used here, discussions of different JSC values will focus primarily on the magnitude of the value and treat it as a positive number, a higher JSC corresponds to a higher J_{ph} [1].

II.1.3 Fill Factor

While VOC and JSC mark the boundaries of power production in a solar cell, the maximum power density produced P_{max} occurs at the voltage V_{max} and current-density J_{max} where the product of J and V is at a minimum (or maximum in absolute value). Because of the diode behavior and additional resistance and recombination losses, $|J_{max}|$ and V_{max} are always less than $|J_{SC}|$ and VOC respectively.

$$FF = \frac{J_{max}V_{max}}{J_{sc}V_{oc}} \quad (\square.1)$$

FF is an indication of how close J_{max} and V_{max} come to the boundaries of power production of JSC and VOC and also an indication of the sharpness of the bend in the exponential J-V curve that connects JSC and VOC. Since higher FF is related to higher maximum power, high FF is

desired. however, the diode-like behavior of solar cells results in FF always being less than one.Devices with high $|J_{SC}|$ and V_{OC} can still have low FF,suggesting that something must be done to improve device quality[2].

II.1.4 Quantum Efficiency

The most discussed performance parameter of a solar cell is the power conversion efficiency η and is defined as the percentage of incident irradiance I_L (light power per unit area) that is converted into output power. Because the point where the cell operates on the J-V curve changes depending on the load, the output power depends on the load. For consistency, the maximum output power is used for calculating efficiency. In equation form, efficiency.

the calculation is:

$$\eta = \frac{|J_{max}| \times V_{max}}{I_L} \times 100\% = \frac{FF \times V_{oc} \times |J_{sc}|}{I_L} \times 100\% \quad (\square . 2)$$

This form clearly shows that FF, J_{SC} , and V_{OC} all have direct effects on η . Furthermore, the area used to calculate J_{sc} affect η and should include inactive areas that are integral to the solar Cell, I_L (light power per unit area) that is converted into output power[3].

II .2 Simulation and optimization of solar cell

Optoelectronic devices have gotten a lot of press in recent years since they're important parts of the Internet and other optical systems such as photovoltaics.Computer simulation is difficult due to the intricacy of physical mechanics in such systems.For performance analysis and design optimization, this is a must-have tool.Throughout the years,there have been various modeling tools created specifically for thin-film PV devices ,alot of these tools have matured and are now available to PV users.

Community Engineers and scientists can use these technologies to construct and comprehend complex systems.nanostructure devices with ever-increasing sophistication .The wide range of materials and devices Selecting physical mechanisms and modeling methodologies might be tricky,theoretical models or software packages that are adequate[4].

II.2.1 Definitions

II.2.1.1 Simulation

Simulation is carried out to determine the impact of certain layer material electrical, optical, and geometric characteristics on total cell performance[5].

- Imitative portrayal of the operation of one system or process through the operation of another.
- Studying a problem that isn't amenable to experimentation.

II.2.1.2 Optimization

Optimisation is carried out by determining the best value for all input parameters based on a wide range of individual input parameter variation and overall cell performance[5].

II.2.2 Simulation and optimization of softwares

In this section, we'll go through some of the current numerical simulation tools for thin-film solar cells. There are many more numerical simulation programs in use than the ones mentioned here[4].

II.2.2.1 AMPS

AMPS stands for Analysis of Microelectronic and Photonic Structures, is a popular simulation tool[6]. It was designed to be a very general and versatile computer simulation tool for device physics and design study. It is a one-dimensional (1D) device physics code that may be used to simulate any two-terminal device, including photovoltaics. Prof. Stephen Fonash and a group of his students at The Pennsylvania State University created AMPS. Prof. Fonash's book has several instances of how AMPS might be employed, along with explanations of the physics[7].

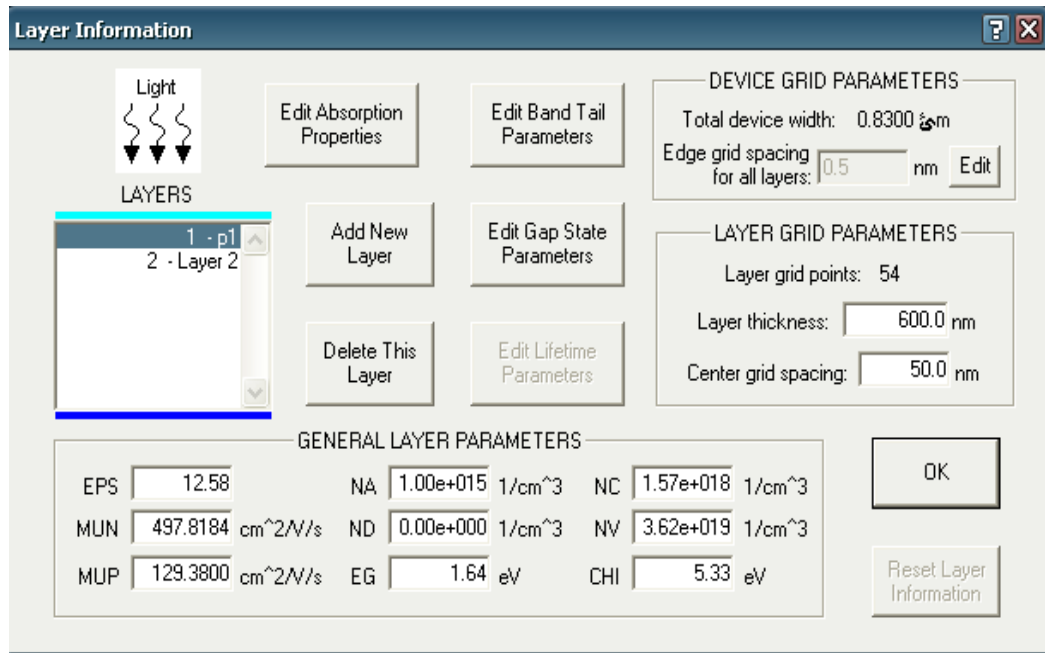


Figure II. 1: Picture of AMPS Program .

II.2.2.2 wxAMPS

wxAMPS is a new program developed in collaboration with the University of Illinois at Urbana-Champaign and Nankai University in China[8]. It is based on the AMPS physical principle. The wxAMPS user interface is cross-platform and allows for quick data entering and excellent visualization. wxAMPS adds two tunneling models and a new algorithm that combines the Newton and Gummel methods to the original AMPS kernel. More detailed simulation of multi-junction solar cells is now achievable because to the addition of a trap-assisted tunneling model, modeling is possible because the simulation allows for an endless number of levels. In wxAMPS, graded solar cells are simple to implement[9].

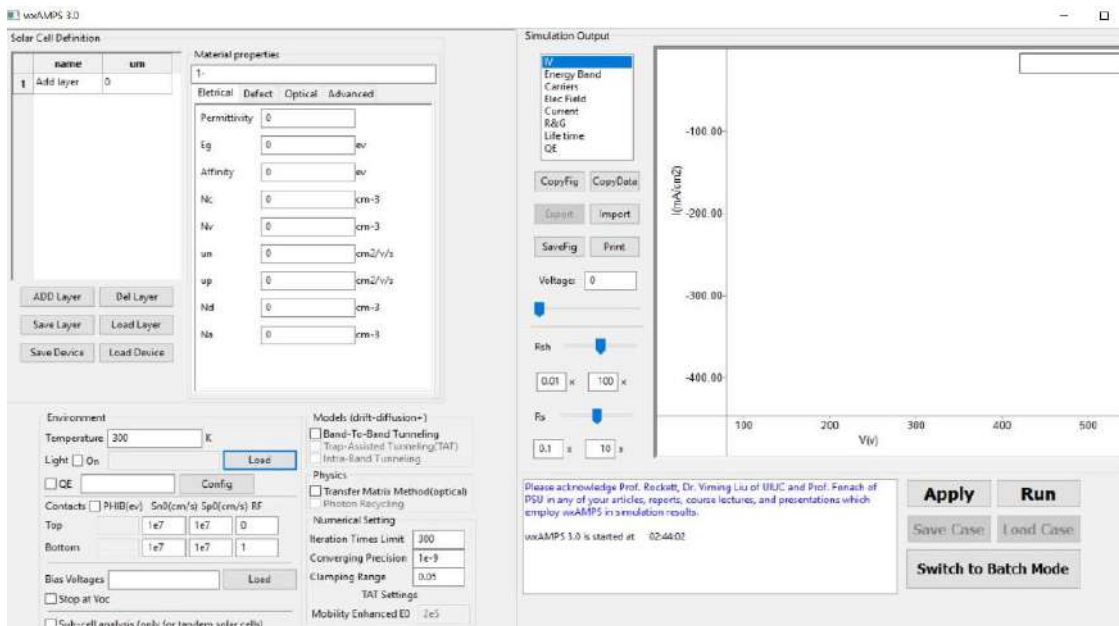


Figure II. 2: Picture of wxAMPS program.

II.2.2.3 PC1D

Basore and coworkers wrote a program for IBM-compatible personal computers that solves the fully coupled nonlinear equations for the quasione-dimensional transport of electrons and holes in crystalline semiconductor devices, with a focus on photovoltaic devices[10].It was originally written at Sandia National Laboratories⁹ and was further developed at UNSW, Australia[4].The commercially accessible solar cell modeling software PC1D is the most often used.Its popularity stems from its quickness, user friendliness, and constant updates to the most recent cell models.It's used to test new devices and to teach new users about device physics.

The University of NSW has made PC1D freely available.More PC1D resources, including a batch file generator, are available at PV Lighthouse[10].PC1D is limited to one-dimensional cell modeling, Basore et al. created PC2D, a circular reference solar cell device simulator, as a result of this.PC2D is a revolutionary silicon solar cell device simulator that completely simulates 2D effects in a Microsoft Excel spreadsheet.The iterative solution of cell formulas with circular references is used to implement the semiconductor drift-diffusion equations for electrons and holes.This 2D simulator is a suitable partner to PC1D thanks to its familiar spreadsheet user interface and open-source access.A selective-emitter cell, an emitter wrap-through cell, and an interdigitated back-contact cell are all examples of device simulations[11].

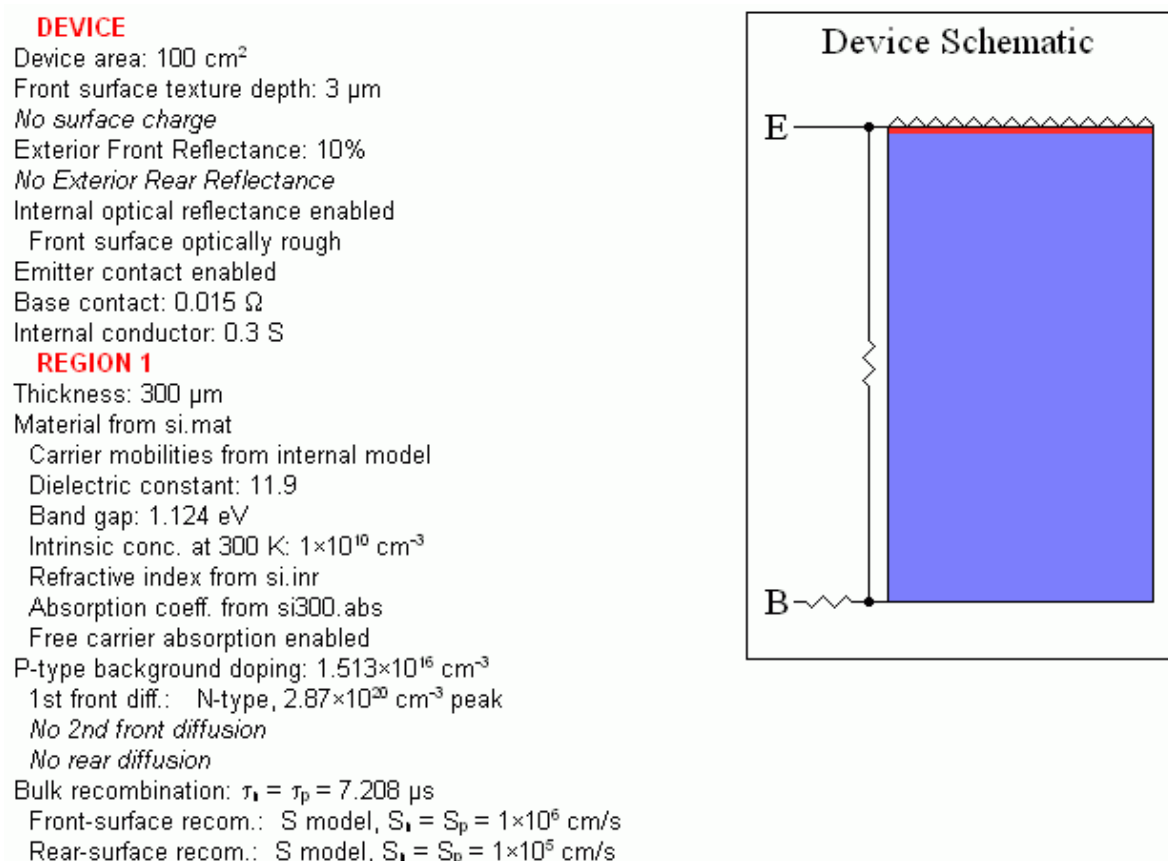


Figure II. 3: Main window of PC1D.

II.2.2.4 AFORS-HET

AFORS-HET (automat for simulation of heterostructures) is a one-dimensional numerical computer program for modeling multilayer homo-or heterojunction solar cells and several popular solar cell characterization methods[12].The program solves the one-dimensional semiconductor equations in steady-state as well as for tiny sinusoidal ac-perturbations.A range of popular characterization techniques,such as current-voltage (IV),internal quantum efficiency (IQE), impedance, capacitance (CV, CT), static surface photovoltage (SPV), electron beam induced current (EBIC), and photoluminescence, have also been employed (PL). A user-friendly interface makes it simple to change parameters, visualize, and compare your simulation[13].The numerical device simulator AFORS-HET was used to model and implement carrier transport through a tunnel barrier, allowing the tunnel current to be calculated.The model is then utilized to study innovative tunnel oxide-based hole collector designs[14].

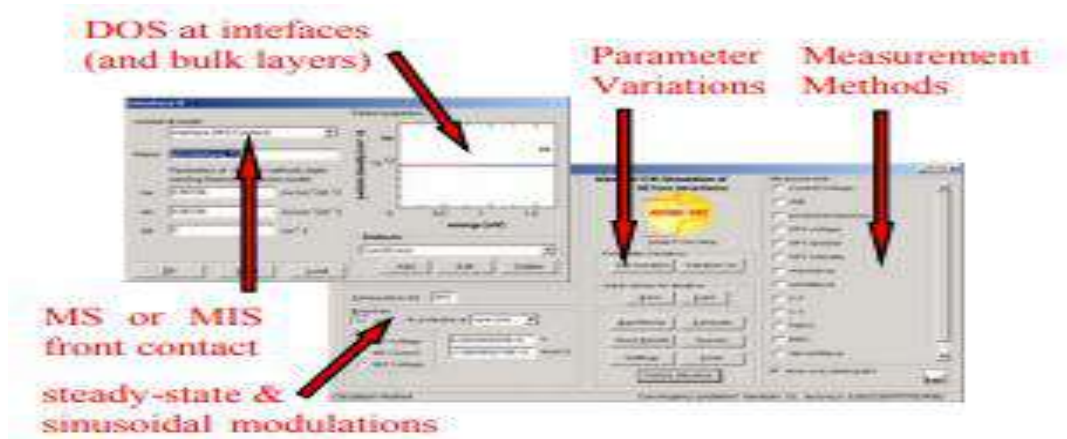


Figure II. 4: graphical interface of AFORS-HET.

II.2.2.5 ASA

Prof Miro Zeman's group at the Technical University of Delft in the Netherlands created ASA (Advanced Semiconductor Analysis) as modeling software designed for amorphous silicon solar cells[15]. ASA can simulate both the spatially resolved generation rate and the electrical transport and recombination of charges in a multilayer system with a distribution of sub-gap defects using a transfer matrix formalism. ASA reads in scripts that contain the input parameters. As a result, external programming languages or tools such as Matlab can be used to update variables in these scripts allowing external scripts to manage the entire product. This versatility enables users to use ASA in novel ways that are unrelated to the original application of amorphous Si solar cells as in ref[16].

II.2.2.6 SCAPS 1D

SCAPS 1D is a one-dimensional solar cell device simulator created at the University of Gent's Electronics and Information Systems (ELIS)[17]. The PV research community can use SCAPS for free. A solar cell can be described as a stack of up to seven layers with variable thicknesses, optical absorption, doping, defect densities, and defect dispersion. Then you may mimic a variety of typical metrics including I-V, QE, C-V, and C-f. SCAPS now supports graded solar cells[18]. As of version 2.8. Each layer's position-dependent composition y can be set using a number of interpolation laws: $y(x)$. These interpolation principles can also be used to determine the composition dependency of all significant semiconductor properties in a layer, the most important of which is the semiconductor conductivity.

The band-gap $E_g(y)$ and the electron affinity are the most important features (y). $E_g(x) = E_g[y(x)]$, for example, when both of them are coupled with the composition profile $y(x)$. In fact, you can grade up to eighteen different attributes. For the Ga-Al-As material system, a specific interpolation approach for optical absorption has been designed and tested[18].

II .3 Simulation and Optimization by SCAPS

II.3.1 Basics

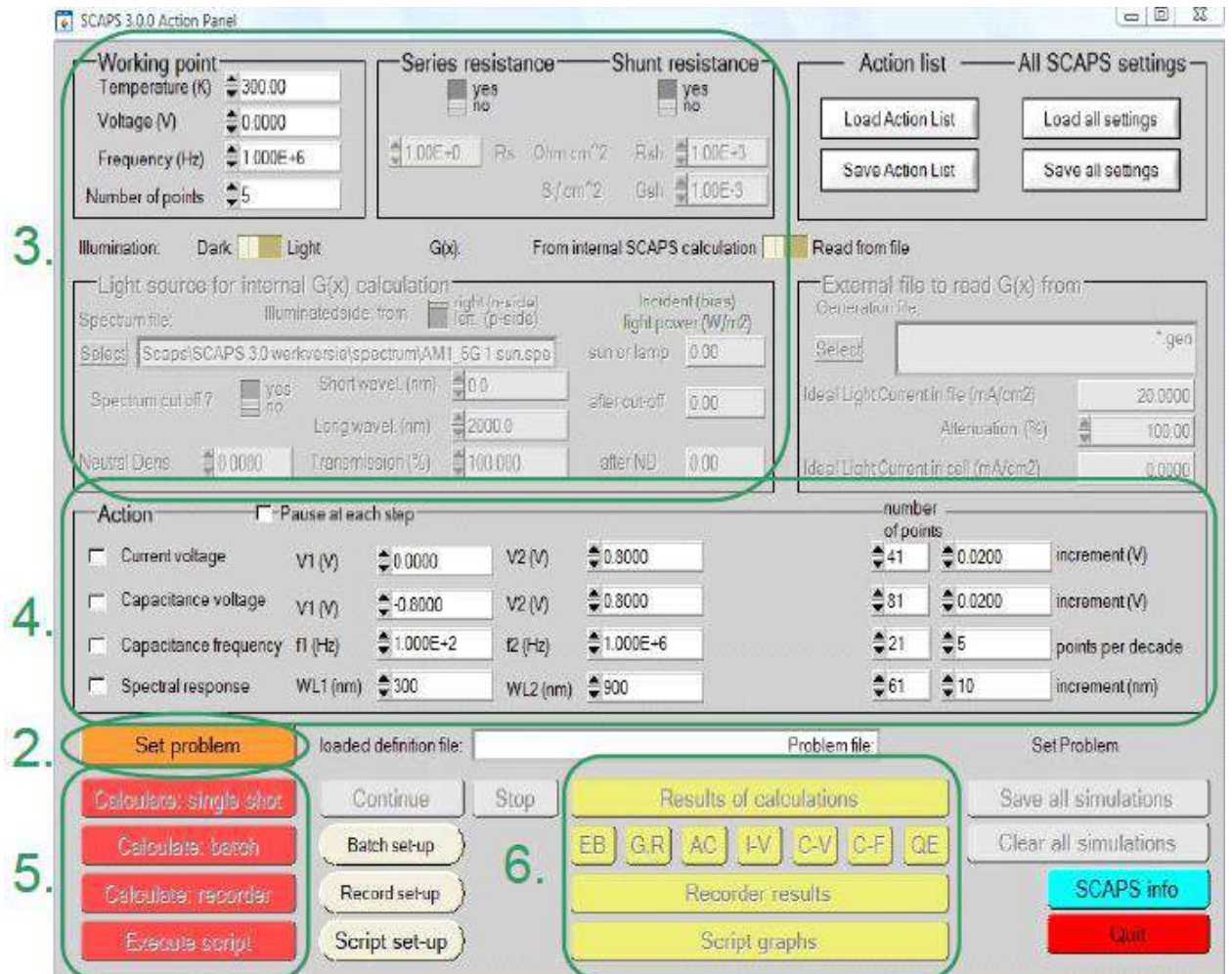


Figure II. 5: The SCAPS start-up panel: the Action panel or main panel.

The meaning of the blocks numbered 1 to 6 is explained as follow

1-Run SCAPS.

2-Define the problem, thus the geometry, the materials, all properties of your solar cell .

3-Indicate the circumstances in which you want to do the simulation, i.e. specify the working point .

4-Indicate what you will calculate, i.e. which measurement you will simulate .

5-Start the calculation(s) .

6-Display the simulated curves.

II.3.2 Conditions of scaps

II.3.2.1 the temperature T

All measurements are applicable. Note that the only variables in SCAPS that have an explicit temperature dependency are $NC(T)$, $NV(T)$, the thermal velocities, the thermal voltage kT , and all associated derivatives: you must input the materials characteristics for each T manually [19].

II.3.2.2 the illumination

For all measures, is utilized. It defines the bias light conditions for the QE measurement. The basic options are dark or bright, lighted side selection, and spectrum selection. The default lighting is one sun ($= 1000 \text{ W/m}^2$) with the 'air mass 1.5, global' spectrum, although you have a vast selection of monochromatic light and spectra for your customized simulations. If you have access to an optical simulator, you can load a generation profile instead of utilizing a spectrum right away [19].

II.3.3 Define the problem

Click the button `set problem` in the action panel, and chose `load` in the lower right corner of the panel that opens. Select and open e.g. the file `CdTe -base` Based on the CdTe-base case by Markus Gloeckler, Colorado, summer 2003 See also: M. Gloeckler, A. Fahrenbruch and J. Sites, "Numerical modelling of CIGS and CdTe solar cells: setting the baseline", Proc. 3rd World Conference on Photovoltaic Energy Conversion (Osaka, Japan, may 2003), pp. 491-494, WCPEC-3, Osaka (2003).



Figure II. 6: Define the working point:

II.3.4 Select the measurement(s) to simulate

You can replicate one or more of the following measures in the action-part of the Action Panel: I-V, C-V, C-f, and QE. Adjust the argument's start and end values, as well as the number of steps, if necessary. Do one simulation at a time at first, using coarse steps: your computer and/or the SCAPS application may be slower than you expect, or your problem may be particularly difficult.

II.3.5 Start the calculation(s)

In the action panel, click the button calculate: single shot. The computations begin when the Energy Bands Panel appears. A status line, such as is from 0.000 to 0.800 Volt: $V = 0.550\text{Volt}$, appears at the bottom of the Panel, indicating how the simulation is progressing.

Meanwhile, SCAPS offers a free video depicting the evolution of the conduction and valence bands, Fermi levels, and the full shebang. You have the right to be angry when you get the dreaded divergence notification, but don't go overboard. In any case, the I-V points you had computed were not lost.

II.3.6 Display the simulated curves

SCAPS shifts to the Energy band panel after the calculation(s) (or the AC-band panel). You may now look at your ease to the band diagrams, carrier densities, current densities, and so on at the final bias point determined (if you want to look at an intermediate state at ease, halt your calculations early or use the pause button on the Action Panel). The results can be printed, saved as graphs, exhibited (numbers are displayed on screen; cut and paste to e.g. Excel is available), or saved (numbers are saved to a file). If you have already simulated at least one related measurement, you can move to one of the specific output Panels. We merely offer the IV Panel as an example.

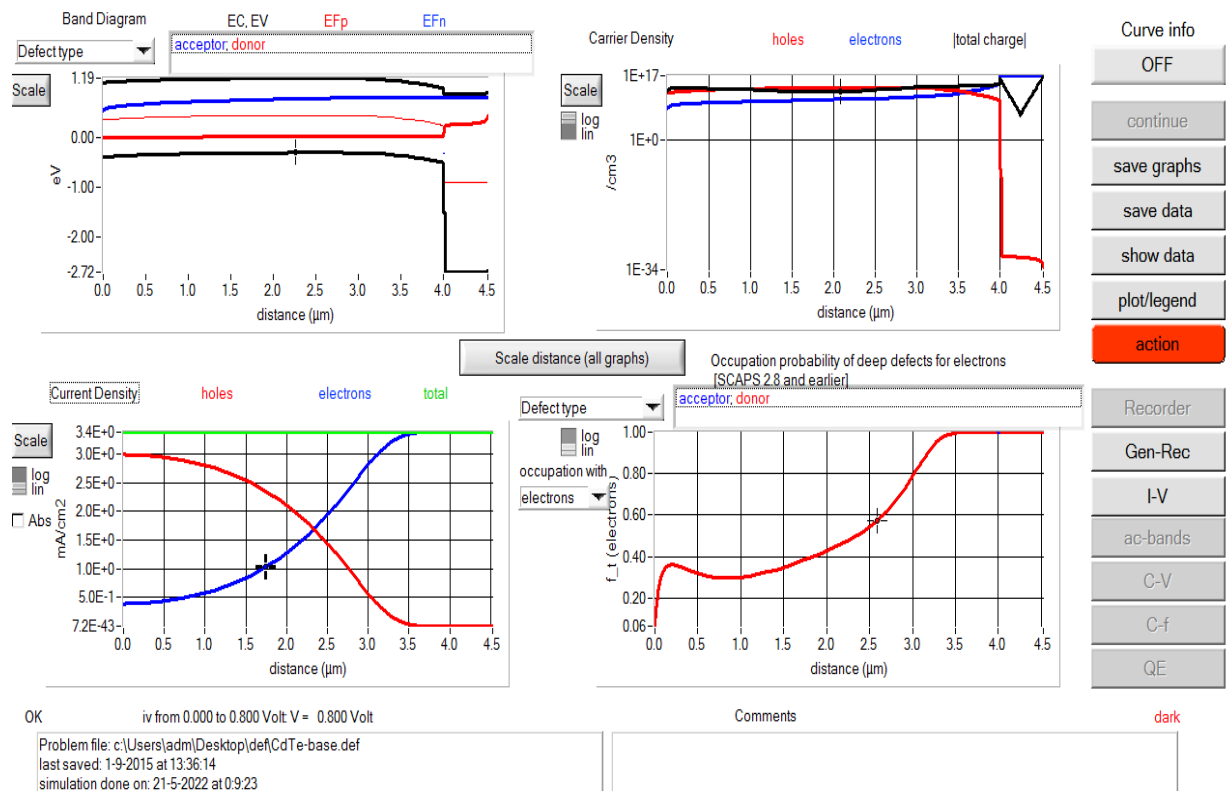


Figure II. 7: Scaps panels.

II.3.7 Editing the problem

Set the problem in the Action Panel. The Solar Cell Definition Panel is now open. When you click on a layer name, the Layer Properties Panel appears, where you may alter all of the layer's properties. Use your instincts and/or continue reading this handbook.

II.3.8 Speeding up: Batch calculation

The batch option is useful when you wish to investigate the impact of one or a few factors on solar cell properties. When you select Batch set-up, a panel appears, allowing you to specify which parameter to alter, over what range, and in what mode (Lin, Log or custom). You may also set many parameters and change them all at once (in a nested or 'simultaneous' manner), but start small. When the button calculate: batch is pressed, a batch computation is started [19].



Figure II. 8: Batch calculation.

II.3.8.1 Speeding up: Recorder

The detailed panels are only available at the last measurement point in a standard single shot or batch calculation. You may run a record computation to view them as a function of the batch parameters. By choosing Record set-up, you should first pick the attributes you wish to keep track of. Look through the property lists, and don't forget to put a property into the recorder list using one of the insert buttons. A recorder computation is started by selecting calculate: recorder. Cell parameters are changed according to the Batch setup, and all simulations required to determine the requested attributes are run. This indicates that the action panel's specified metrics are disregarded [19].

II.3.9 Editing a solar cell structure

The Solar cell definition window appears when you click the Set Problem button on the action panel. This panel allows you to construct and edit solar cell structures, as well as save and load definition files. These definition files are ordinary ASCII files with the extension .def that may be

viewed using a text editor such as notepad. Even though the format of these files appears self-explanatory, it is highly cautioned against manually altering them [19].

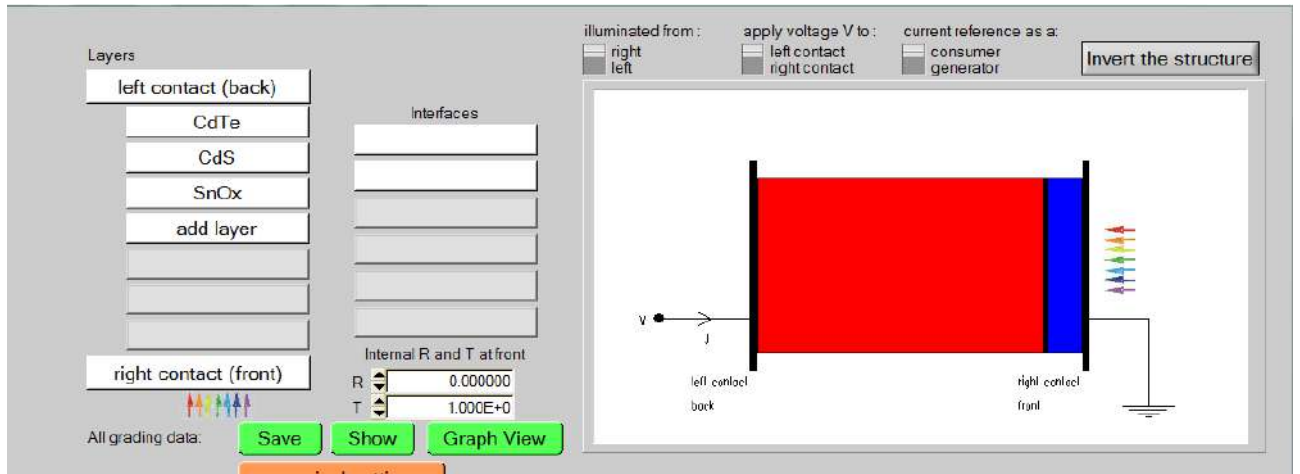


Figure II. 9: Defining a solar cell structure.

II .4 Measurement specific options

II.4.1 The IV-panel

The results of the current-voltage simulations are shown on the IV-panel. The left graph displays all I-V simulations. The right graph gives detailed information about the recombination currents in the last simulation. This allows to see the main recombination mechanism in the structure for varying voltages. If the simulation is performed under illumination, the solar cell parameters are calculated and shown, see Figure 10. If SCAPS needed to perform an extrapolation to determine these parameters, the warning LED below the parameter turns red. As most users set the voltage range from $V_{start} = 0$ to some V_{stop} , the need for extrapolation will first show up for V_{oc} and thus FF (if $V_{stop} < V_{oc}$, when the references for voltage are such that both are positive numbers). When the voltage is more restricted, $V_{stop} < V_{mpp}$ (mpp is the maximum power point), then also extrapolation is needed to determine the efficiency. When V_{start} was set to 0 (the default value), J_{sc} will be determined precisely (no interpolation or extrapolation needed). When extrapolation was needed, and when SCAPS deems the result not physical, both the extrapolated (but unreliable) parameter and the warning LED are not shown. This is the case if SCAPS would find $V_{oc} < 0$ or $V_{oc} > 10$ Volt (we do not believe in supermegagigantic good solar cells...). So, if some of your solar cells parameters do not show up (e.g. you see J_{sc} and but not V_{oc} and FF), just extend your voltage range to include V_{oc} , and do not immediately start to harass us with e-mails about ‘malfunctions’ in SCAPS1. As already mentioned, when the generation was ‘from file’, no efficiency can be calculated, but the collection efficiency is given instead [20].

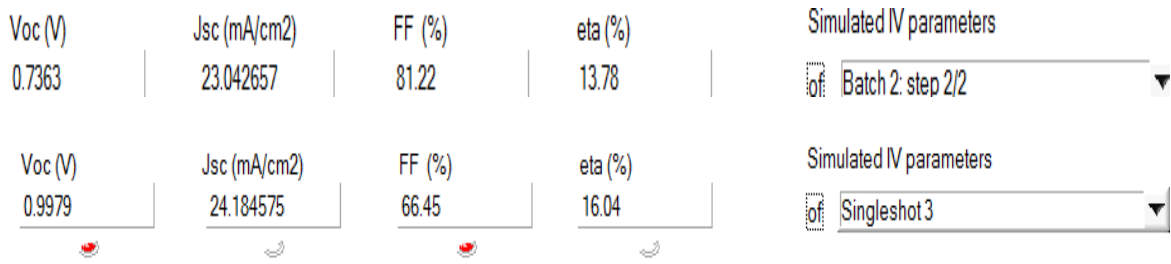


Figure II. 10: Examples of visualization of the solar cell parameters Voc, Jsc, FF and eta.

II.4.2 The CV-panel

This panel displays the capacitance and conductance as a function of applied voltage. Moreover, a MottSchottky diagram and the apparent doping density are calculated. In order to calculate this apparent doping density profile, a numerical differentiation of the data is needed together with a choice of the relative permittivity. These options can be set by clicking the Analysis method-button, which opens the Admittance (capacitance) analysis panel[19].

II.4.3 The QE-panel

This panel allows to analyze the QE simulations. Specifically, the meaning of QE in SCAPS is external quantum efficiency QE: the number of electrons leaving the cell (ass current) divided by the total number of photons incident on the cell. On the horizontal axis one can display either the wavelength or the photon energy of the monochromated light. On the vertical axis one has a wider choice:

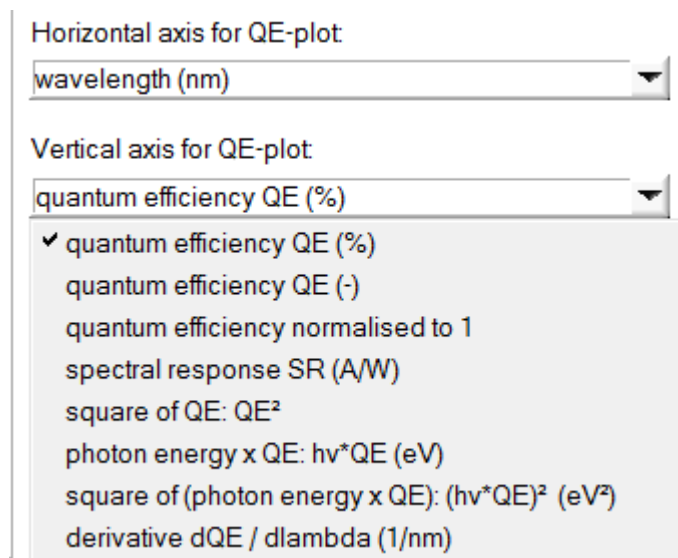


Figure II. 11: Ordinate choices on the QE-panel.

III .1 CdTe over time

Thin film polycrystalline CdTe based solar cells are one of the most promising candidates for photovoltaic energy conversion because of their potential to realize low cost, high efficiency, reliable and stable thin film solar cell. To begin with, the cell is made of polycrystalline materials and glass, which are potentially less expensive than other counter components. Second, CdTe has a high absorption coefficient, which means that all the incident photons with energy greater than the bandgap can be absorbed within the first few microns of thickness of CdTe absorber layer. CdTe has a direct optical bandgap of 1.5eV which is very close to the optimum bandgap for solar cells. The thickness required for an absorption layer makes the cost of material for CdTe solar cells relatively low. One of the primary goals of today's solar cell research is to use less semiconductor material while making the cells thinner. Thinning will not only save material, but it will also minimize recombination loss, cut production time, and reduce the amount of energy required to make solar cells. All of these elements will lower the cost of production. Furthermore, CdTe thin film solar cells have demonstrated long-term stability and excellent efficiency under AM1.5 illumination for extra terrestrial use and stannic oxide (SnO_2) and silver (Ag) has been considered as the anode and cathode of the CdTe/CDS solar cell respectively. However, conversion efficiencies of homojunction CdTe solar cells have not shown encouraging results. Thus, heterojunction cells structure with wide band-gap n-type semiconductor (commonly CdS) and p-type CdTe are widely used. Moreover, from the optoelectronic and chemical properties, CdS is the best suited n-type heterojunction partner to CdTe for high efficiency and low cost cells. The maximum theoretical efficiency for CdTe band gap (1.5 eV) and a standard solar spectrum is about 29%. In 1982, Tyan published an interesting paper on CdTe/CdS thin film solar cells reporting an efficiency of 10% [1]. Afterwards, an efficiency of 16.04% has been reached by Ferekides. Finally a group of NREL researchers reported a record efficiency of 16% [2]. This champion 16% efficient CdS/CdTe cell used modified cell structure of CdS/CdTe with 0.025 μm CdS and 4 μm CdTe layer fabricated using three different technology CSS for CdTe film, CBD for CdS film and magnetron sputtering for all other layers [3].

There is a little over half of the 29% theoretical limit, but it was estimated that practical CdTe devices with 18–19% efficiencies should be feasible in the near future[4]. However, there are scopes to improve the CdS/CdTe solar cell performance further more by modified design and simple deposition technique to improve one of cell output parameters. Low open circuit voltage (V_{oc}) has been recorded in CdS/CdTe cells compared to its counterparts. The V_{oc} , where the value of the record CdTe cell is roughly 230 mV below the GaAs cell, makes the most contribution to the efficiency differential with the same bandgap material like GaAs. When compared to crystalline silicon, the similar voltage differential for the second primary thin-film polycrystalline solar cell. If the CdTe voltage deficit was reduced to the same 30 mV, with the same current and fill factor, CdTe cells would achieve the efficiency about 16%. In practice, the voltage may further be compromised by higher carrier density ($\sim 10^{16} \text{ cm}^{-3}$) and higher absorber lifetime (more than 1ns) as well as by reducing the significant back-contact barrier height. The strategies for improving voltage and cell performance have been explored utilizing *AMI_5G 1 sun.spe* simulator and have also been thoroughly discussed in this work.

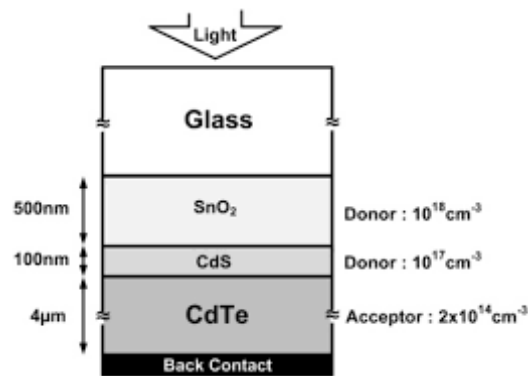


Figure III. 1: Structure of the CdS/CdTe,As solar cells studied[20].

III .2 Device Modeling and Simulation

The traditional CdTe baseline case structure is shown in (fig III. 1), as well as the modified (Glass/ SnO_2)/CdS/CdTe/Ag) CdTe cell structure for better conversion efficiency (η). The new structure contains an additional layer (SnO_2) between the TCO and the CdS layer to generate an ultra-thin CdS window layer for higher performance and a thinner CdTe layer, as shown in (fig III. 1). As a result, the front contact is made up of TCO and a buffer layer. which is more effective and practical to achieve today. Because of the low cost, silver

(Ag) is utilized as the back contact material in the modified structured cell, with a back contact barrier height (bL) of 1.25 eV instead of Au (bL= 0.4 eV). Solar cell simulation could be beneficial in terms of saving time and money[5]. In this work, *scaps* simulator was used to explore the conventional CdTe baseline cell and modified structured cells for achieving thinner CdTe and CdS layers with higher conversion efficiency. This *scaps* program has been developed to realistically simulate the electrical characteristics of the thin-film heterojunction solar cells. It has been tested for thin-film CdTe and CIGS solar cells[6]. We study the current density–voltage (J-V) characteristic of the cell (figure III. 2). The short-circuit current density (J_{sc}) of 24.18 mA/cm², open-circuit voltage (V_{oc}) of 0.99 V, fill factor (FF) of 66.45%, and power conversion efficiency (PCE) of 16.04% are obtained. The simulated device performance is consistent with the experimental values of the Tin-based PSCs, certifying that the device simulation is valid and the input parameters that have been set are close to those for a real device. The optical absorption edge of tin perovskite is red-shifted to 900 nm in the external quantum efficiency (QE) curve (see fig III. 2). The QE covers the entire visible spectrum and reaches a broad absorption maximum over 50% from 400 nm to 850 nm accompanied by a notable absorption on set up to 950 nm, which is in good accordance with the measured QE spectrum[7]. The red-shift of the QE curve is more beneficial to the light absorption at infrared wavelengths.

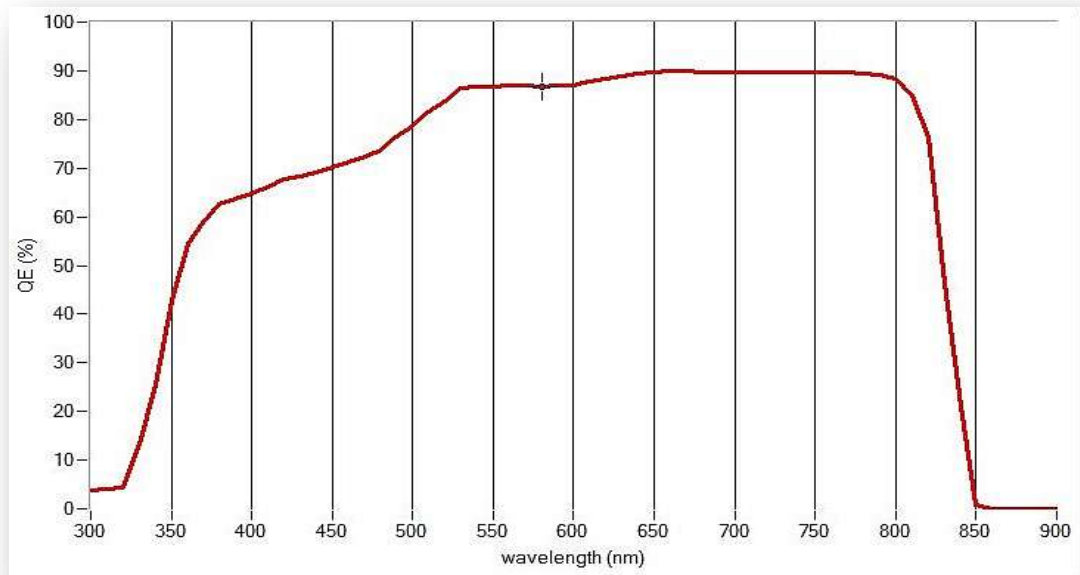


Figure III. 2: Effect of CdTe thickness on the quantum efficiency.

In the Table III.1, some of the properties of CdTe and CdS thin films are given as used while doing simulation of CdS/CdTe solar cells. Typical electrical parameters for CdTe / CdS films[8].

| Layers parameters | CDTE | CDS | SNO _x |
|---|------------------|--------------|------------------|
| <u>Thickness (μm)</u> | 4.00 | 0.025 | 0.500 |
| Bandgap (eV) | 1.50 | 2.400 | 3.600 |
| <u>Electron affinity (eV)</u> | 3.900 | 3.700 | 4.000 |
| Dielectric permittivity (relave) | 9.400 | 10.000 | 9.000 |
| Electron mobility(cm²/V-s) | 3.200E+2 | 2.200E+18 | 2.2000E+18 |
| Hole mobility (cm²/V-s) | 4.000E+1 | 1.800E+9 | 1.800E+9 |
| Electron density (cm⁻³) | 1.000E+7 | 1.000E+7 | 1.000E+7 |
| Hole density (cm⁻³) | 1.000E+7 | 1.000E+7 | 1.000E+7 |
| Donor density ND (1/cm³) | 0.000E+0 | 1.1000E+18 | 1.000E+17 |
| acceptor density NA (1/cm³) | 2.000E+14 | 0.000E+0 | 0.000E+0 |

The donor concentration will depend strongly on the deposition method, but a desirable value of $2.000E+14 \text{ cm}^{-3}$ is given here. If this value could be increased to $3.000E+14 \text{ cm}^{-3}$ by some doping process we could expect better results for the solar cell open circuit voltage[8].

III .3 Results and discussion

III .3.1 Influences of thiknees of CdTe

Numerical modeling tools can aid knowledge of solar cells and provide additional suggestions for modifying structure and cell parameters to increase cell performance. In the particular solar cell model, there are more than 50 parameters that can be changed [9]. A issue with 50 variables is obviously too confusing to be solved reliably. As a result, it's vital to keep the number of variable parameters to a minimum by setting several of them to "acceptable" values. Choosing the suitable parameters was a difficult task. Many of them are dependent on fabrication and deposition procedures, and so vary amongst devices. The calculations in this paper begin with a three-layer device model of a SnO₂/CdS/CdTe solar cell. thinner and more efficient cells. in this work, first of all the conventional CdTe baseline structure (SnO₂/CdS/CdTe) has been investigated and a conversion efficiency of 16.04% ($V_{oc} = 0.99$ V, $J_{sc} = 24.18$ mA/cm², FF = 66.45) was found with 3 μ m CdTe absorber layer. It has been found that the conversion efficiency increases up to 16.14% ($V_{oc} = 0.85$ V, $J_{sc} = 24.11$ mA/cm², FF = 75.71).

To date, practically all high-efficiency CdTe solar cells have been made with a CdTe layer that is greater than 5 μ m thick. However, more numerical analysis has been done with the goal of lowering the thickness of the CdTe and CdS layers in CdS/CdTe solar cells to save material and expense. The thickness of the CdTe layer has been changed from 1 μ m to 5 μ m to investigate a thinner absorber layer, and the simulation results are presented in (fig III. 3).It is clear from that all the solar cell output parameters are almost constant above the CdTe thickness of 2 μ m. The short circuit current density (J_{sc}) and V_{oc} ,QE slowly decreased between 2 and 1 μ m but the FF remained unaffected by the reduction of CdTe thickness until 1 μ m, but below 1 μ m of CdTe thickness The short circuit current density (J_{sc}) and V_{oc} ,QE are decreased drastically, which has shown good agreement with similar works [10].As a result , the efficiency showed increased between 1 to 3 μ m which indicates that 3 μ m is the optimal value CdTe thickness when the efficiency are high value.

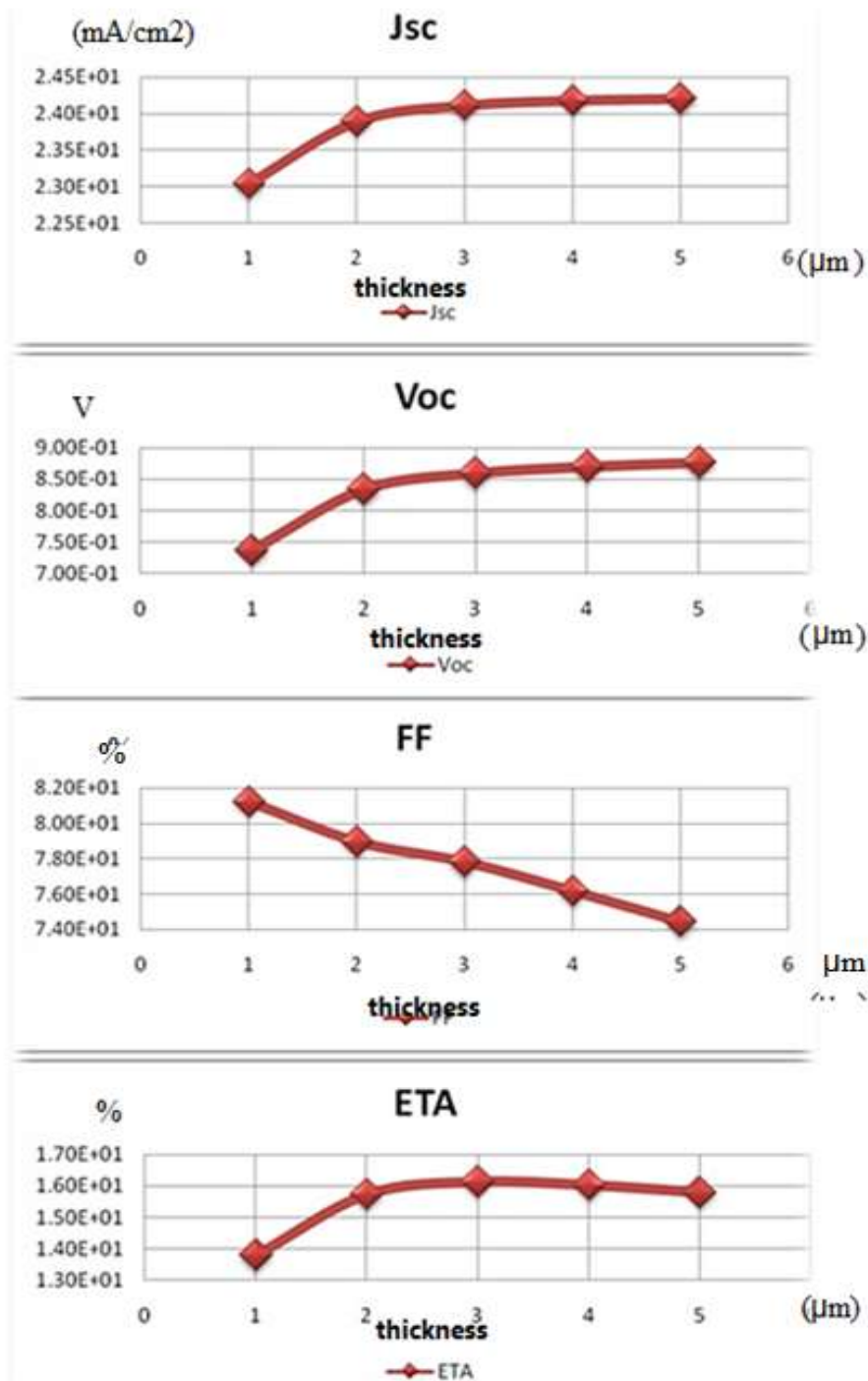


Figure III. 3: Effect of the CdTe film thicknesses on cell performance.

A conversion efficiency of 16.11% ($V_{oc} = 0.87$ V, $J_{sc} = 24.11$ mA/cm², $FF = 77.90$) has been achieved for 3 μm thick CdTe cell, These results are in good agreement with related published results by others on CdTe cells [11]. The QE of CdTe layer thickness variation from 5 nm to 50 nm is shown in (Fig III. 4).

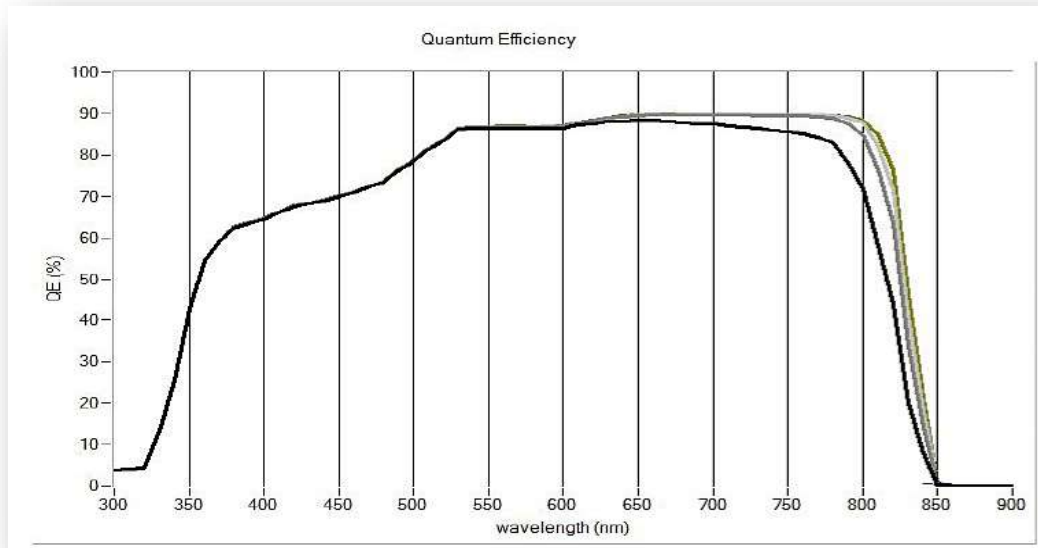


Figure III. 4: Effect of CdTe thickness on the quantum efficiency.

III.3.2 Influences of thiknees of CDS

When the CdS film thickness has been reduced to explore thinner CdS layer, the absorption loss in the blue region due to thick CdS layer also reduces, which improves mainly J_{sc} and consequently the efficiency (fig III. 5) shows the effects in details of CdS layer reduction from 5 nm to 25 nm on the cell parameters such as J_{sc} , V_{oc} , FF and η from *AMI_5G 1 sun.spe* simulation, with CdTe layer thickness of 1 μm and CdS layer thickness of 10 nm. (fig III. 5) shows that J_{sc} has improved greatly with reduced CdS layer with no effect on V_{oc} and a little decrease in FF. As a result, η increased with reduced CdS layer. The QE of CdS layer thickness variation from 5 nm to 25 nm is shown in (fig III. 6). As can be seen, when the wavelength is below 510 nm the quantum efficiency is much affected with the increasing CdS layer thickness and finally the conversion efficiency. These results are in good agreements with other literatures [12],[13]. However, to date, it is impractical to fabricate good quality devices with CdS film thickness below 5 nm by process that has been selected for the fabrication of this layer. For fabrication limitation we have selected the CdS film thickness of 5 nm with η of 16.78% ($V_{oc} = 0.872$ V, $J_{sc} = 25.52$ mA/cm², FF = 0.762). The η improvement achieved is mainly due to the improvement in J_{sc} .

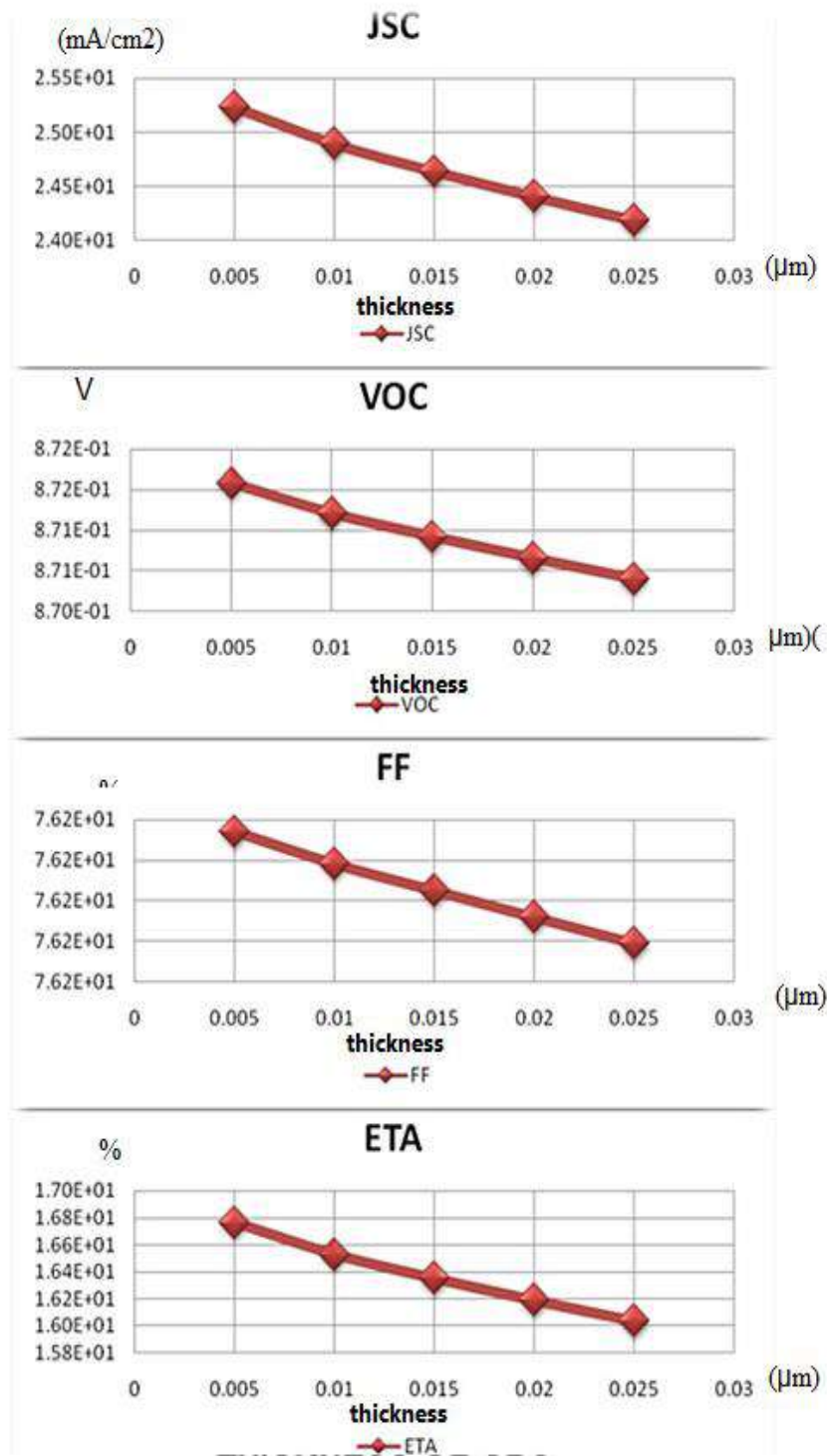


Figure III. 5: Effect of the CDS film thicknesses on cell performance.

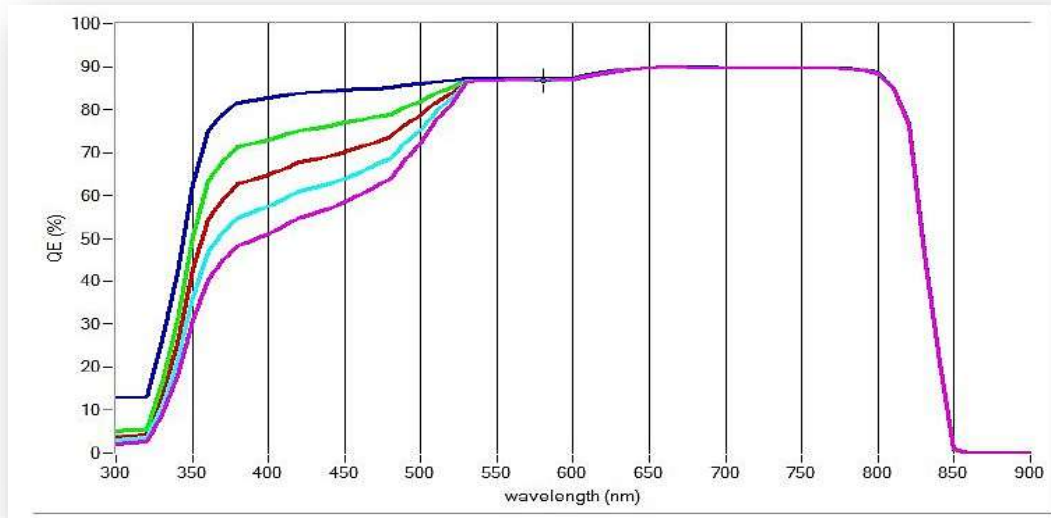


Figure III. 6: Effect of CdS thicknesses on the cell QE.

III .3.3 Influences of electron affinity of CDS

The band offset between CDS/CdTe layers is a decisive factor of carrier recombination at the interface, which determines the open-circuit voltage (V_{oc}). The band offsets are adjusted by varying the values of electron affinity (χ) of the CDS (3.3 eV–3.7 eV). The variations of J_{sc} , V_{oc} , FF, and PCE with electron affinity value are shown in (fig III. 7). A better solar cell PCE can be obtained at the χ values of 3.3 eV–3.7 eV for the buffer. A barrier cliff is formed at the absorber interface as shown in the inset of (fig III. 7). The proper electron barrier cliff around 0.0 eV–0.2 eV does not affect the photo-generated electron flow toward a back electrode, and J_{sc} is almost constant. When the E_c -CDS is more than 3.5 eV higher than E_c -absorber, the collection of electrons is impeded by the raised barrier formed at the conduction band offset (see fig III. 7). This is because of the double-diode like curvature at higher conduction band offset [14],[15].

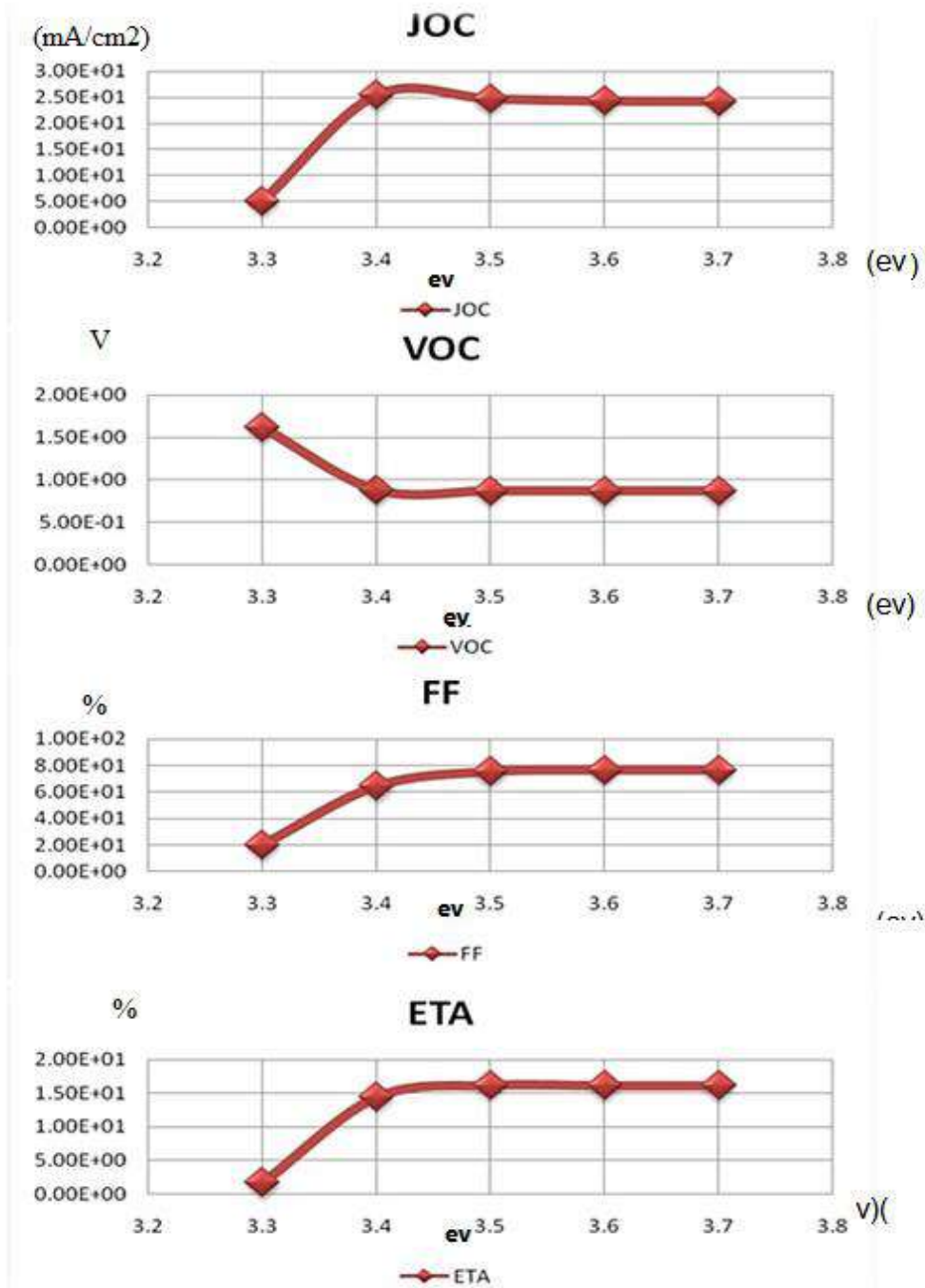


Figure III. 7: Effect of the CDS electron affinity on cell performance.

The optimum properties of the solar cell of PCE of 16.15%, J_{sc} of 25 mA/cm², V_{oc} of 0.99 V, and FF of 79.80% are obtained when the electron affinity values of the CDS are set to be 3.5 eV. Obvious improvement of the voltage-current characteristics can be seen from the J–V curves with the band offset optimization (see curve 3 in fig III. 7). The simulation results of the electron affinity of CDS are similar to those from the band offset study on CdTe[14].

III.3.4 The Influences of acceptor concentration of CdTe layer

The acceptor concentration (N_A) derived from $C-V$ measurements for As concentrations ranging from $6 \times 10^{13} \text{ As cm}^{-3}$ to $7 \times 10^{14} \text{ As cm}^{-3}$ is shown in (fig III. 8). The layers were grown under Cd-rich conditions, with a CdTe precursor ratio of 2 to facilitate As incorporation. Increasing this ratio to 4, the highest achievable N_A increased only marginally (from 2×10^{14} to $7 \times 10^{14} \text{ cm}^{-3}$) with no noticeable change in the activation ratio [16]. WD estimated from these profiles (fig III. 8 inset) confirms an inverse power dependence between the two parameters. Overall, these results show that px CdTe films with small grains can be effectively doped, similar to large CdTe crystals [17][18].

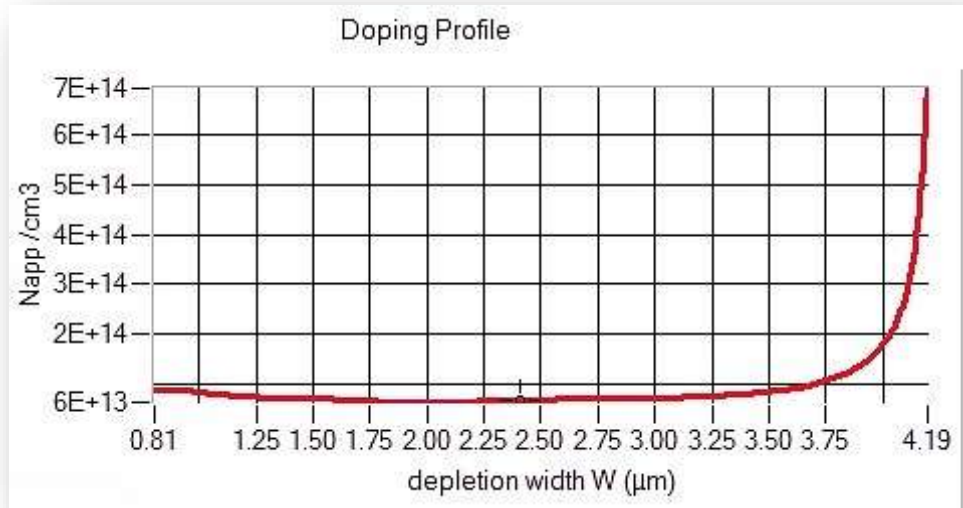


Figure III. 8: Acceptor concentration (N_A) profile for px CdTe samples produced by *in-situ* doping with As concentration increasing from $6 \times 10^{13} \text{ As cm}^{-3}$ (bottom profile) to $7 \times 10^{14} \text{ As cm}^{-3}$ (top profile).

In order to make it clear how the acceptor doping concentration (N_A) of the perovskite absorption layer can affect the performances of solar cells, CdTe layers with the values of N_A ranging from $1 \times 10^{14} \text{ cm}^{-3}$ to $3 \times 10^{14} \text{ cm}^{-3}$ are considered. (fig III. 9) provides the PCEs of solar cells with different acceptor densities of the perovskite. The J_{sc} and V_{oc} are also related to the change of N_A for the perovskite, and both of them reach their maximum values when the N_A is approximately $3 \times 10^{14} \text{ cm}^{-3}$. The external quantum efficiency (QE) significantly increases with the N_A of perovskite (see fig III. 10), which implies that the generation rate of the photo-generated carrier increases under the same incident photon

number. Hence, an appropriate doping concentration of the perovskite absorption layer is beneficial to the improvement of the photo-absorption efficiency and the J_{sc} . However, the J_{oc} drops rapidly when the NA exceeds $1 \times 10^{14} \text{ cm}^{-3}$. The variation in the cell performance with the doping concentration can be explained from the perspective of the built-in electric field which is enhanced with the increase of doping concentration. The enhancement of the electric field promotes the separation of carriers and then the improvement of the cell performance. However, further increasing the doping concentration will cause a higher Auger recombination rate, which is not beneficial to the increase of V_{oc} . It can be found from (fig III. 10) the hole transportation will be greatly suppressed with the increase of p-type doping concentration of the perovskite absorption layer because of the enhanced impurity scattering and recombination.

The quasi Fermi level of the hole (E_{Fp}) becomes far from the valence band top with the increase of NA, even flattens into the E_{Fp} of the HTM. This affects the hole transportation strongly from the absorption layers to HTM, and the reduction of the hole density can also be seen from the E_{Fp} uplift of the perovskite absorption layer. The optimum properties of the solar cell of PCE of 16.41%, J_{sc} of 24.05 mA/cm^2 , V_{oc} of 0.883 V, and FF of 77.40% are obtained when the acceptor concentration values of the CdTe are set to be $3 \times 10^{14} \text{ cm}^{-3}$.

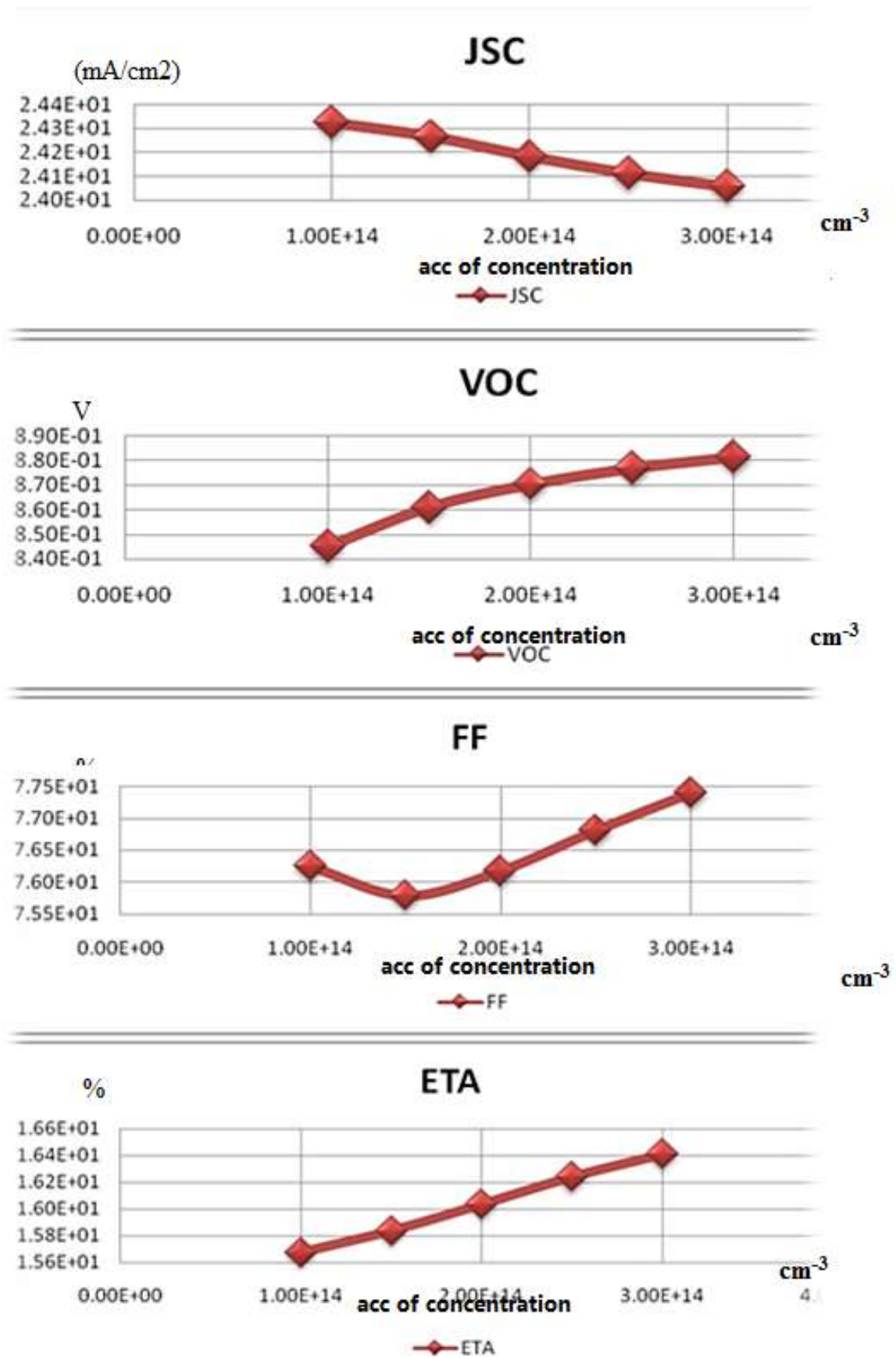


Figure III. 9: Effect of the CdTe film acceptor concentration on cell performance.

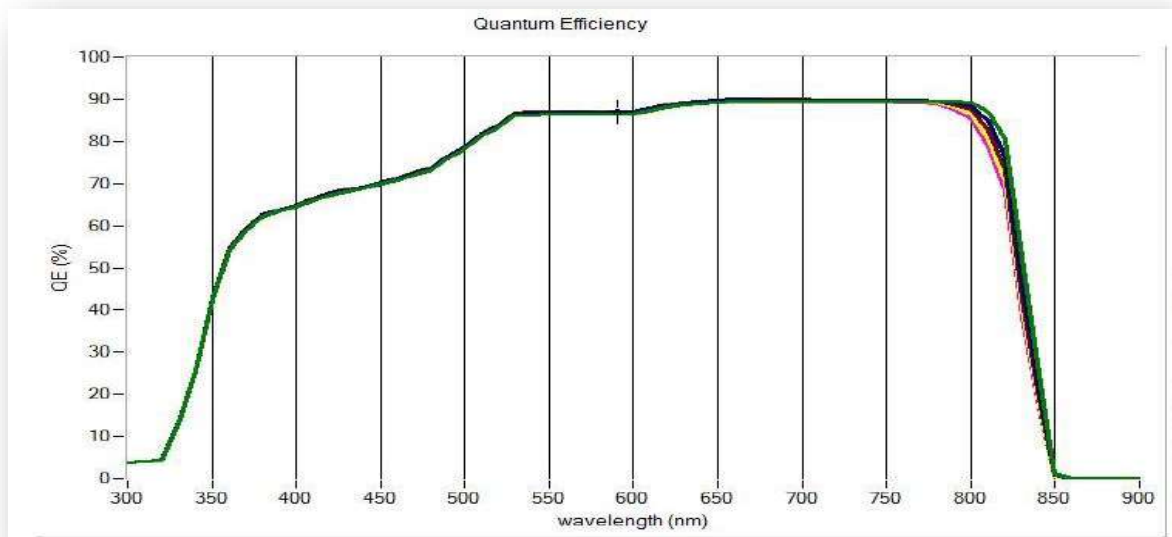


Figure III. 10: Effect of CdTe acceptor concentration on the cell QE.

In this tables we put the parameters of original case performance of CdTe/CDS thin film solar cell, and the new parameters we obtained after optimization of thin film solar cells.

Table III. 1: Original case Performance of CdTe/CDS thin film Solar Cell.

| PARAMETERS | PERFORMANCE | | | |
|-----------------------------------|--------------------------|--------|-------|---------|
| | JSC(mA/cm ²) | VOC(V) | FF | ETA (%) |
| THICKNESS OF CDTE=4μm | 24.18 | 0.99 | 66.45 | 16.04 |
| THICKNES OF CDS=0.025μm | | | | |
| ELECTRON AFFINITY=3.7eV | | | | |
| ACCEPTOR CONCENTRATION =2.000E+14 | | | | |

Table III. 2: Performance of CdTe/CDS thin film Solar Cell for varying CdTe layer thickness.

| THICKNESS OF CDTE | JSC(mA/cm ²) | VOC(V) | FF | ETA (%) |
|-------------------|--------------------------|--------|-------|---------|
| 3 μm | 24.11 | 0.87 | 0.779 | 16.11 |

Table III. 3: Performance of CdTe/CDS thin film Solar Cell for varying CDS layer thickness.

| THICKNESS OF CDS | JSC (mA/cm ²) | VOC (V) | FF | ETA (%) |
|------------------|---------------------------|---------|-------|---------|
| 0.005 μm | 25.52 | 0.872 | 0.762 | 16.78 |

Table III. 4: Performance of CdTe/CDS thin film Solar Cell for varying CDS layer electron affinity.

| ELECTRON AFFINITY | JSC- (mA/cm ²) | VOC (V) | FF | ETA (%) |
|-------------------|----------------------------|---------|-------|---------|
| 3.5 ev | 25 | 0.99 | 0.798 | 16.15 |

Table III. 5: Performance of CdTe/CDS thin film Solar Cell for varying CdTe layer acceptor of concentration.

| ACCEPTOR CONCENTRATION | JSC (mA/cm ²) | VOC (V) | FF | ETA (%) |
|--|---------------------------|---------|-------|---------|
| $3 \times 10^{14} \text{ cm}^{-3}$ | 24.05 | 0.883 | 0.774 | 16.41 |

After analyzing the simulation of THIN FILM solar cells with varying thickness, electron affinity and acceptor concentration, it has been found that, enhanced absorption of the charge carriers at the active layer of the cell can be achieved with decreasing the thickness of the active layer, due to less recombination effect, which consequently increases the output electrical power and QE. We find Quantum Efficiency of 16.04% for thickness of 4 μm , 16.78% for CDS thickness of 0.005 μm , 16.15% for CDS electron affinity 3.5 eV and 16.41% for acceptor concentration $3 \times 10^{14} \text{cm}^{-3}$. Finally, the charge concentration profile at the cell active layer and the gradient of the profile has been studied. Regarding the carrier concentration profile, we found that, the gradient of the charge carriers increases with increasing the electron affinity and acceptor concentration at the CdTe/CDS active layer.

CONCLUSION

In this work, the performance parameters of the CdTe/CDS thin film Solar cell have been analyzed by studying the characteristics of the layers. The characteristics of the CdTe/CDS cell have been studied with varying the layer thickness, electron affinity and acceptor concentration. Each of these cases, the form factor (FF) , external quantum efficiency (EQE) of the layers has been determined and analyzed. The simulation has been performed under the consideration of incident solar radiation of 1kW/m^2 irradiance and Air mass of 1.5 and stannic oxide (SnO_2) and silver (Ag) has been considered as the anode and cathode of the CdTe/CDS solar cell respectively. Here, the voltage, current circuit, Fill Factor (FF) and External Quantum Efficiency (EQE) of the solar cell has been determined for layer thickness of $4\mu\text{m}$ CdTe, $0.005\ \mu\text{m}$ CDS, electron affinity of 3.5 eV, acceptor concentration of $3 \times 10^{14}\text{cm}^{-3}$. From the simulation of the work, it has been concluded that, highly efficient CdTe/CDS thin film solar cell can be produced if the active layer is properly fabricated with thickness and also with high acceptor concentration and enhanced electron affinity. In this work, we find External Quantum Efficiency of 16.14% for thickness of $4\mu\text{m}$, 16.53% for CDS thickness of $0.005\ \mu\text{m}$, 16.15% for CDS electron affinity 3.5 eV and 16.41% for acceptor concentration $3 \times 10^{14}\text{cm}^{-3}$.

Bibliography

Reference of chapter 1

- [1] <https://www.intechopen.com/chapters/52325>.
- [2] H. Frey and H. R. Khan, *Handbook of Thin-Film Technology*. .
- [3] Technology_thin_film__hand_flexing.
- [4] Edn. Cambridge University Press Born M, Wolf E (2003) Principles of optics, “Principles of optics.”
- [5] B. N. (1992) E. and polarized light. N.-H. Azzam RMA, “Ellipsometry and polarized light.”
- [6] Peter m. Martin, deposition technologies for films and coatings. 2002.
- [7] Edn. Springer MacAdam DL (1985) Color measurement, “Color measurement.”
- [8] R. D. V. I. role for Humans, “Metal Ions in Life Sciences,” no. ;13:139-169. DOI: 10.1007/978-94-007-7500-8_5 [.
- [9] L. F. and S. R. Edited by László Nánai, Aneeya Samantara, “Methods for Film Synthesis and Coating Procedures.”
- [10] https://www.academia.edu/45566626/evaluation_of_thermal_performance_on_a_stand_alone_pv_solar_inverter, “evaluation of* thermal performance on a stand alone pv solar inverter.”
- [11] https://www.researchgate.net/profile/Nicolas_Wyrsh/publication/12872592_Photovoltaic_Technology_The_Case_for_ThinFilm_Solar_Cells.
- [12] <https://www.science.org/doi/10.1126/science.285.5428.692>, “No Title.”
- [13] A. date: 19. 12. . [Http://ideaenerji.com/Flexible%20.html](http://ideaenerji.com/Flexible%20.html), “No Title.” .
- [14] T. Geremew, “Review of Thin Film Deposition Technique and Its Application AUTHOR’S Temesgen Geremew Tefery Bule Hora University, Department of physics, Bule Hora, Ethiopia Corresponding author E-mail:,” 2021.
- [15] https://www.researchgate.net/publication/276423464_Solar_Cells_review, “Solar_Cells_review.”
- [16] Ç.Şule, “Photovoltaic power generation for polycrystalline solar cells and turning sunlight into electricity.”

- [17] A. S. Shiva Gorjian, P. I. 9780128196106, and eBook I. 9780128226414, “Photovoltaic Solar Energy Conversion.”
- [18] [Http://solarbotics.net/starting/200202_solar_cells/200202_solar_cell_types.html](http://solarbotics.net/starting/200202_solar_cells/200202_solar_cell_types.html), “solar_cell_types.html.”
- [19] [Https://www.sciencedirect.com/science/article/pii/S0306261911002790](https://www.sciencedirect.com/science/article/pii/S0306261911002790).
- [20] N. D. Tobnaghi DM, Madatov R, “The effect of temperature on electrical parameters of solar cells.”
- [21] G. B. N. dyes for dye sensitized solar cell:] Richhariya G, Kumar A, Tekasakul P and A. Review., “Natural dyes for dye sensitized solar cell: a review.”
- [22] P. of the 14th E. J. Merten, J. M. Asensi, A. Shah, J. Andreu, “Commission Photovoltaic Solar Energy Conference.”
- [23] H. rishard stanford unversity. Bube, “photovoltaic materials.”

Reference of chapter 2

- [1] N. MESSEI and D. on: 12 / 06 / 2016, “Study of the effect of grading in composition on the performance of thin film solar cells based on AlGaAs and CZTSSe, a numerical simulation approach.”
- [2] R. F. (1996). Pierret, “Semiconductor device fundamentals. New York: Addison- Wesley Publishing Company, Inc.”
- [3] J. William J. Potscavage, “‘Physics and Engineering of Organic Solar Cells’ , Georgia Institute of Technology, May, 2011.”
- [4] S. D. & P. N. M. Burgelman, J. Verschraegen, “Modeling Thin-film PV Devices, Prog. Photovolt: Res. Appl, 11:1–11(2003).”
- [5] S. Selberherr SpringerVerlag/Wien (1984)., “, Analysis and Simulation of Semiconductor Devices,.”
- [6] [Https://www.researchgate.net/publication/276423464_Solar_Cells_review](https://www.researchgate.net/publication/276423464_Solar_Cells_review), “Solar_Cells_review.”
- [7] S. F. second edition-A. press (2010)., “Solar Cell Device Physics,.”
- [8] D. H. & A. R. 37th I. (2011). Y. Liu, “Photovoltaic Specialists Conference (PVSC),.”
- [9] Doi:10. 1016/j. solmat. 10. 01. (2011) . “Photovoltaic Specialists Conference. ”

- [10] <https://www.engineering.unsw.edu.au/ener-engineering/pc1d-software>10.04.2016, “formodelling-a-solar-cell.”
- [11] I.:2156-3381 (2011) P. A. Basore & K. Cabanas-Holmen, IEEE Journal of Vol 1, 7277, “Photovoltaics ,.”
- [12] C. L. and J. H. S. E. I. 978-953-307-052 (2010). R. Stangl, “Numerical Simulation of Solar Cells and Solar Cell Characterization Methods: the Open-Source on Demand Program AFORS-HET, R. D. Rugescu (Ed.),.”
- [13] 3rd World Conference on A. Froitzheim, R. Stangl, M. Kriegel, L. Elstner & W. Fuhs, Proc. WCPEC-3, “Photovoltaic Energy Conversion, Osaka, Japan, 1P-D3-34 (2013).”
- [14] R. Varache, C. Leendertz, M. E. Gueunier-Farret, J. Haschke, D. Muñoz & L. Korte, j.solmat 141 , 14–23(2015).
- [15] J. K. J. M. R. 23:889 (2008). M. Zeman, “[Optical and electrical modeling of thin-film silicon solar cells,.”
- [16] J. C. (eds) V. B. H. (2014) D. Beljonne, “Multiscale Modelling of Organic and Hybrid Photovoltaics-Springer,.”
- [17] M. Burgelman, P. Nollet & S. 527, “Degrave, Thin Solid Films,.”
- [18] S. 2151-2155(2008). M. Burgelman, J. Marlein Valencia, Spain 2151-2155(2008). Valencia, “Proceedings of the 23rd European Photovoltaic Conference, [.”
- [19] S. D. Marc Burgelman Koen Decock, Alex Niemegeers, Johan Verschraegen and V. 18-12-2020, “SCAPS manual.”
- [20] J. Marlein, M. Burgelman 28-30 March 2007). p. 227-233 2007, “, Proceedings of NUMOS (Int. Workshop on Numerical Modelling of Thin Film Solar Cells, Gent (B).”

Reference of chapter 3

- [1] E. . Tyan, Y.S., PerezHALbuerne, “Efficient thin film CdS/CdTe solar cells, Proceedings of 16th IEEE Photovoltaic Specialists Conference, IEEE Publishing, New York, 1982, p. 794. [.”
- [2] L. Ferekides, C., Britt, J., Ma, Y., Killian, ““High efficiency CdTe solar cells by close spaced sublimation’, Proceedings of Twenty ThirdPhotovoltaicSpecialistsConference IEEE, New York, USA, 1993, p. 389.”

- [3] pp. 803–814 Xuanzhi Wu, “High efficiency polycrystalline CdTe thinHfilm solar cells”, Solar Energy, 2004, 77, “HighHefficiency polycrystalline CdTe thinHfilm solar cells”, Solar Energy.”
- [4] J. R. S. M. Gloeckler, A. L. Fahrenbruch, “Proceedings of the 3rd World Conf. on Photovoltaic Energy Conversion (2003), p. 491.”
- [5] P. 133H137. F. Jahanshah, K. Sopian, H. Abdullah, I. Ahmad, M. Y. Othman, S. H. Zaidi, Proceedings of the 7th WSEAS International Conference on WAVELET ANALYSIS & MULTIRATE SYSTEMS (WAMUS '07), Arcachon, France, October 13H15, 2007, “ANALYSIS & MULTIRATE SYSTEMS.”
- [6] P. of 3rd W. S. Degrave, M. Burgelman, and P. Nollet, “Conference on Photovoltaic Energy Conversion, 2003, pp. 47H 50. [.]”
- [7] S. R. 2009 J. Appl., “Phys. 105104505.”
- [8] AZAMI ZAHARIM3 AND KAMARUZZAMAN SOPIAN M. A. MATIN1, NOWSHAD AMIN1, “A_study_towards_the_possibility_of_ultra - THINFILM CDS/CDTE.”
- [9] P. M. Burgelman, J. Verschraegen, S. Degrave and P. Nollet, “Photovoltaics, 143 (2004).”
- [10] M. Y. and A. Z. Nowshad Amin, Kamaruzzaman Sopian, “Proceedings of the 8th WSEAS International Conference on POWER SYSTEMS (PS 2008), Santander, Cantabria, Spain, September 2325, 2008, pp.299.”
- [11] M. K. N. Amin, T. Isaka, T. Okamoto, A. Yamada, “Jpanese Journal of Applied Physics 38 (1999) 4666.”
- [12] A. E. A. N. A. Hasan Afifi, M. AbdelH Naby, Said ElH Hefnawie, “, WSEAS TRANSACTIONS on ELECTRONICS, Issue 4, Volume 2, October 2005, pp 180H184.”
- [13] I. R. S. Mahmud Abdul Matin Bhuiyan, Nowshad Amin and Kamaruzzaman Sopian, “Conference on Research and Development, SCOReD 2008, IEEE, UTM Malaysia, November 26H27, ISBN: 978H1H 4244H2869H4, pageH210.”
- [14] H. S. and S. E. H. 2013 A. Kemp K W, Labelle A J, Thon S M, Ip A H, Kramer I J, “Energy Mater. 3917.”
- [15] H. A. and S. H. J. 2013 Ball J M Lee M M, “Energ. Environ. Sci. 6 1739.”
- [16] K. K. N. S.M. Sze, “Semiconductor Devices Physics and Technology.”

- [17] W. K. M. E. Colegrove, J.-H. Yang, S.P. Harvey, M.R. Young, J.M. Burst, J.N. Duenow, D.S. Albin, S.-H. Wei, “Experimental and theoretical comparison of Sb, As, and P diffusion mechanisms and doping in CdTe.”
- [18] W. K. M. B.E. McCandless, W.A. Buchanan, C.P. Thompson, G. Sriramagiri, R.J. Lovelett, J. Duenow, D. Albin, S. Jensen, E. Colegrove, J. Moseley, H. Moutinho, S. Harvey, M. Al-Jassim, “Overcoming carrier concentration limits in polycrystalline CdTe thin films with in situ doping.”
- [19] 18th International Nowshad Amin, Mahmud A. Matin and Kamaruzzaman Sopian, Prospects of Novel Front and Back Contacts for High Efficiency Cadmium Telluride Thin Film Solar Cells from Numerical Analysis, “Photovoltaic Science and Engineering Conference H PVSECH18, Kolkata, India, January 21H25, 2009.”
- [20] <https://opg.optica.org/oe/fulltext.cfm?uri=oe-22-103-A921>